

Primordial Gravitational Waves From Open Inflation

Martin Bucher^{†1,2} and J.D. Cohn^{‡3}

¹Physics Department, Princeton University
Princeton, New Jersey 08544

²Institute for Theoretical Physics, State University of New York
Stony Brook, New York 11794

³Institute for Cosmology, Physics Department, Tufts University
Medford, Massachusetts 02155

Abstract

We calculate the spectrum of gravitational waves generated during inflation in open ($\Omega_0 < 1$) inflationary models. In such models an initial epoch of old inflation solves the horizon and flatness problems, and during this first epoch of inflation the quantum state of the graviton field rapidly approaches the Bunch-Davies vacuum. Then old inflation ends by the nucleation of a single bubble, inside of which there is a shortened epoch of slow-roll inflation giving $\Omega_0 < 1$ today. In this paper we re-express the Bunch-Davies vacuum for the graviton field in terms of the hyperbolic modes inside the bubble and propagate these modes forward in time into the present era. We derive the expression for the contribution from these gravity waves to the cosmic microwave background anisotropy including the effect of a finite energy difference across the bubble wall. [PACS numbers 98.80Bp, 98.80Cq]

[January 1997]

† Current address: Institute for Theoretical Physics, State University of New York, Stony Brook, New York 11794. E-mail: bucher@insti.physics.sunysb.edu

‡ E-mail: jdc@cosmos2.phy.tufts.edu

1. Introduction

It has been well known for quite some time that gravitational waves are generated during inflation and give an observable, and sometimes substantial, contribution to the cosmic microwave background anisotropy [1-7]. For flat ($\Omega_0 = 1$) inflation the spectrum of gravitational waves generated and their observational consequences have been studied quite extensively. However, for open ($\Omega_0 < 1$) inflationary models in which our entire observable universe lies inside a single bubble [8,9,10,11], there has been no complete calculation of the gravitational waves generated. In this paper we present such a calculation.

Gravitational waves from inflation result from the stretching of quantum vacuum fluctuations of the linearized graviton field to superhorizon scales. Following a given mode of fixed co-moving wavenumber k , one finds that at early times its physical wavelength $\lambda = a(t) \cdot (2\pi)/k$ is much smaller than the Hubble length $\ell_H = H^{-1}$ (i.e., the mode is well within the *horizon*). This implies that for determining a physically reasonable *vacuum state* for the mode at early times, one may ignore the expansion of the universe and match onto the usual flat Minkowski space vacuum for the graviton field. Once the correct quantum vacuum state has been determined at early times, to continue these modes to later times become a mathematically well-defined exercise in classical field theory, which involves propagating the *positive* frequency modes—those associated with annihilation operators of the vacuum—forward in time, through the end of inflation into the present epoch. As a mode crosses the horizon its amplitude becomes frozen in. The process of generating gravitational waves during inflation is quite analogous to the process of generating scalar fluctuations during inflation. There is, however, an important difference. The amplitude of the gravitational waves does not depend on the slope of the potential; rather only the overall height of the potential, or equivalently the expansion rate H during inflation, is relevant. As a first approximation for calculating the gravitational waves, H may be regarded as fixed during the relevant epoch of inflation.

For open inflation identifying the correct initial conditions for the linearized graviton field is not as straightforward as for the flat case, because the underlying spacetime geometry is more complicated. The simplest case involves one matter field, the inflaton ϕ , and minimal coupling to gravity. More complicated models such as found in [12] have similar properties

for the gravity wave calculations done here, so the simple one field model is used in the following description. (For a more detailed discussion of single bubble inflation see [10].)

In the one field models, there is an initial epoch of old inflation during which ϕ is stuck in a false vacuum with $\phi = \phi_{fv}$. During this epoch, the spacetime geometry approaches that of pure de Sitter space, characterized by an expansion rate H_{fv} where $H_{fv}^2 = (8\pi G/3)V[\phi_{fv}]$. During this initial epoch of old inflation the graviton field is driven to the vacuum state. This determines the initial conditions using the same considerations as for the flat case described above. Then old inflation ends through the nucleation of a bubble, which expands roughly at the speed of light. The preferred time slicing inside the light cone of the bubble center corresponds to a spatially open universe. Inside the bubble the inflaton field first slowly rolls down a rather flat part of the potential, giving a shortened epoch of slow-roll inflation inside the bubble. Later inside the bubble, the inflaton field rolls more quickly and the usual reheating occurs, converting the vacuum energy of the inflaton field into radiation and matter.

The coordinate chart with the line element

$$ds^2 = -dt^2 + a^2(t) \cdot [d\xi^2 + \sinh^2[\xi] d\Omega_{(2)}^2], \quad (1.1)$$

describes an expanding Friedman Robertson Walker universe with spatially uniform negative spatial curvature. Hyperbolic open coordinates (rather than the *flat* coordinates, to be described later) are the natural coordinate choice in the presence of the bubble wall, which is why the interior of a bubble is an open universe [8, 9]. For de Sitter space and these hyperbolic coordinates, $a(t) = \sinh[t]$, and

$$ds^2 = -dt_h^2 + \sinh^2[t_h] \cdot [d\xi^2 + \sinh^2[\xi] d\Omega_{(2)}^2] \quad (1.2)$$

where ($0 \leq t_h < +\infty$). The hyperbolic coordinate chart has an unphysical coordinate singularity at $t = 0$, and to determine initial conditions it is necessary to consider a larger region of spacetime than that covered by the open coordinates with the line element (1.1).

The bubble nucleation process underlying open inflation is sketched in Fig. 1, with the dashed lines indicating the surfaces on which inflaton field is constant. Roughly speaking, the

forward light cone of the materialization center M , which we shall call region I and which is covered by the coordinate chart just described, may be considered the bubble interior. Regions II and III cover the spacetime prior to bubble nucleation and the part of spacetime into which the bubble expands, at a speed approaching the speed of light.

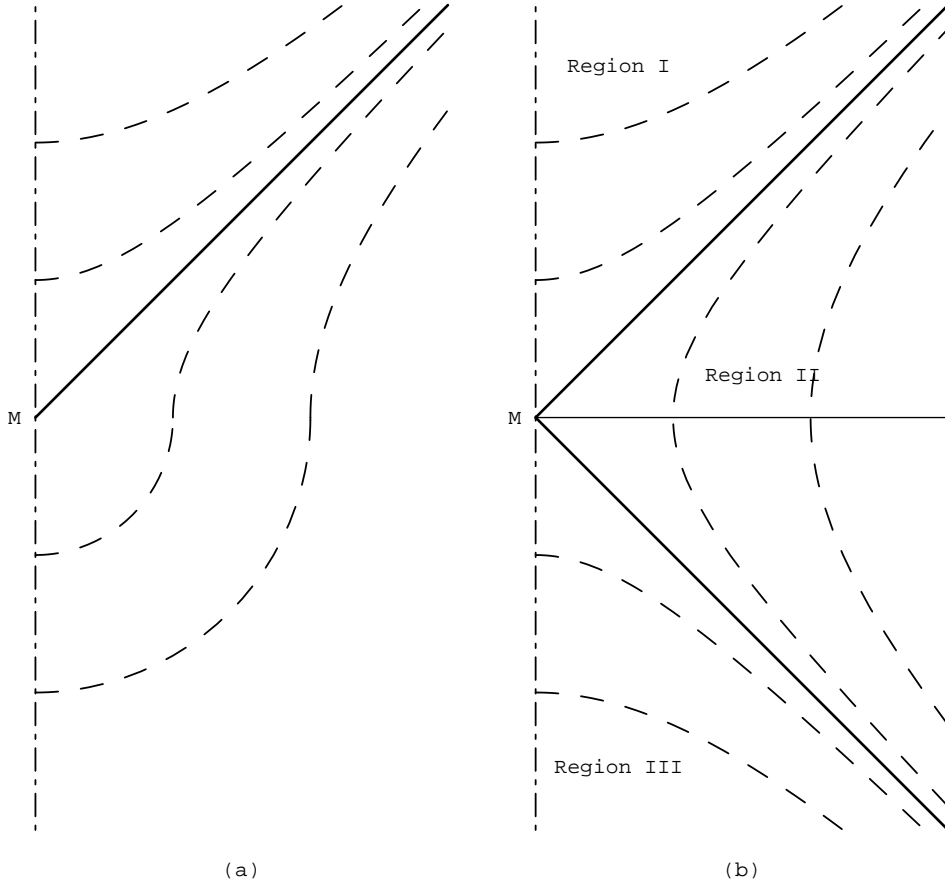


Figure 1—Spacetime Diagram for Open Inflation. Fig. 1(a) shows a spacetime diagram for bubble nucleation. The double-dashed vertical line to the left indicates an $r = 0$ coordinate singularity. Time flows upward and the horizontal axis represents a radial coordinate. On the surfaces represented by dashed curves the inflaton field is constant. The lower portion of the diagram (with $t < 0$) represents the nucleation of a critical bubble, a classically forbidden Euclidean process. For $t > 0$ the bubble expands classically, at a speed approaching that of light. The classical expanding bubble evolution is $SO(3, 1)$ symmetric. In Fig. 1(b) the hyperbolic coordinates that maximally exploit the $SO(3, 1)$ symmetry of the expanding bubble solution are sketched. Spacetime is divided into three hyperbolic coordinate patches. The light cones separating these regions represent unphysical coordinate singularities of a character similar to that of the Schwarzschild horizon.

For future reference, in Fig. 2, we present the conformal diagram for all of maximally

extended de Sitter space. In addition to the regions already mentioned, there also exist regions IV and V, which are the past and future light cones of \bar{M} , the antipodal point of the apex of region I. For a discussion of the global structure of the de Sitter vacuum see [13,14].

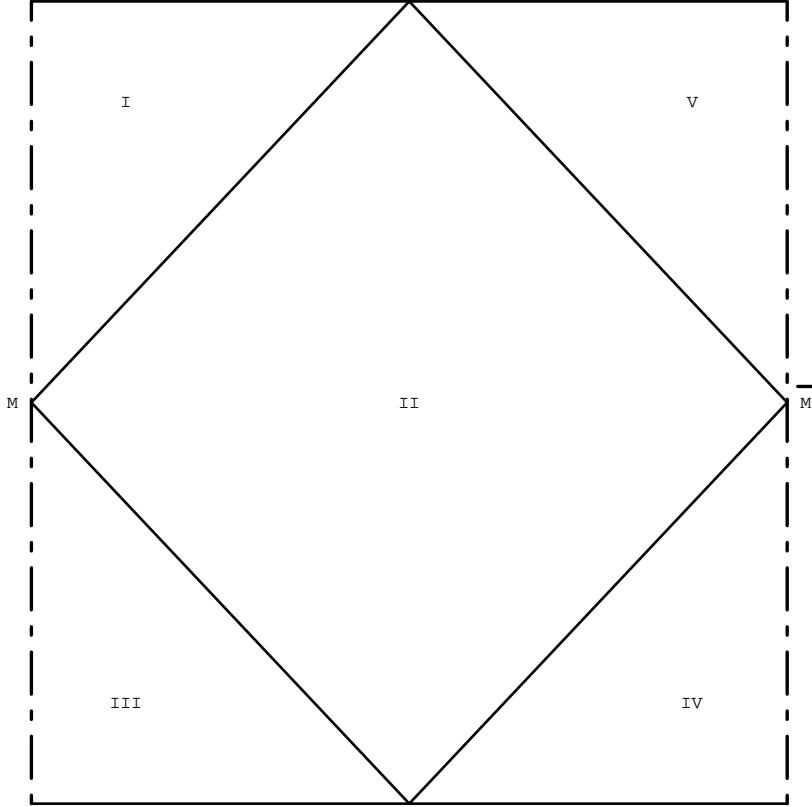


Figure 2—Hyperbolic Coordinates for Maximally Extended de Sitter Space. A conformal diagram for all of maximally extended de Sitter space is shown here. \bar{M} is the antipodal point of M . The hyperbolic coordinates that exploit the symmetry of the $SO(3, 1)$ subgroup of the full de Sitter group $SO(4, 1)$ that leaves invariant M (and \bar{M} as well) divides spacetime into the five indicated coordinate patches.

The subject of *scalar* perturbations in open inflation has been studied extensively in recent years. Lyth and Stewart [15] and Ratra and Peebles [16] calculated the scalar perturbations in open inflation assuming conformal boundary conditions for the vacuum of the inflaton field as $t \rightarrow 0$ in region I. Bucher, Goldhaber, and Turok [10] presented the first computation of the scalar perturbations in open inflation using the Bunch-Davies vacuum for the inflaton field outside the bubble during the prior epoch of old inflation as initial conditions and propagating the scalar modes through the bubble wall into the open universe.

Yamamoto, Sasaki, and Tanaka obtained essentially the same results using Euclidean methods [17, 18]. Many recent calculations of scalar field perturbations, for example [12, 19, 20, 18, 21], take into account additional effects such as finite bubble size, varying bubble wall profile, fluctuations in the bubble wall, *et cetera*.

The subject of gravitational waves generated during open inflation was previously investigated by B. Allen and R. Caldwell in an unpublished manuscript [22]. Within their approximations they found an infrared divergence in the multipole moments of the cosmic microwave background anisotropy (CMB). In their computation, in order to simplify the calculation, at early times a flat spacetime geometry (i.e., that of Minkowski space) is assumed, and to improve the infrared behavior of the graviton field during this early epoch, the graviton field is given a small mass m_g , which at the end of the calculation taken to approach zero. Later on, inside region I on a hyperboloid of constant time with respect to the region I coordinates, the spacetime geometry is taken to change discontinuously to that of de Sitter space. Subsequently, inflation inside the bubble ends, so that the scale factor $a(\eta)$ becomes governed by a radiation-matter equation of state, and the evolution of the graviton field is computed to take into account this change. This is a situation different from open inflation and violates the Einstein equations for the background solution.

In section IV of this paper we derive the Bunch-Davies vacuum for the graviton field in de Sitter space in terms of the hyperbolic region I coordinates, assuming de Sitter space everywhere and a vanishing graviton mass. The Bunch-Davies vacuum for the graviton field in de Sitter space, expressed in terms of the spatially flat coordinate slicing, is used to express the Bunch-Davies vacuum for the graviton field in de Sitter space in terms of the hyperbolic coordinates. The latter are the natural coordinates for studying perturbations in an open universe. While in principle it should be possible to compute directly the transformation between the flat and the hyperbolic modes, in practice this transformation has proven algebraically intractable. Instead, we characterize linear combinations of modes of *positive* frequency with respect to the flat coordinates (which is the same as *positive* frequency with respect to the Bunch-Davies vacuum) in terms of analytic properties in the complex plane. In this way linear combinations of hyperbolic modes of purely *positive* frequency with respect to the Bunch-Davies vacuum may be constructed without explicitly expressing these

combinations in terms of the flat modes. The basic approach is somewhat analogous to the Euclidean methods used by Sasaki et al. for scalar modes [14], except that here, rather than using a Euclidean principle as the starting point, we determine the vacuum in terms of the flat modes, using the complex plane as a mathematical tool.

Our result for the Bunch-Davies vacuum for the graviton field essentially coincides with that found by Allen and Caldwell. There are some minor differences: whereas we obtain a mixed state directly, Allen and Caldwell obtain a pure state, which in the limit $m_g \rightarrow 0$ mocks our mixed state. This does not alter the divergence of the CMB multipole moments.

One caveat in computing the CMB moments relates to gauge fixing. In the Sachs-Wolfe formula for the CMB anisotropy the gravity waves contribute only in the integral along the line of sight—there is no contribution from the *tensor* modes from the last scattering surface. Since linearized gauge transformations are *scalar* and *vector*, one would think that the *tensor* part is gauge invariant.[‡] However, gauge transformations can move the last scattering surface, and thus change the *intrinsic* contribution in the Sachs-Wolfe formula. If gravity wave modes mix with pure gauge modes, cancellations may occur [23]. Linearized gravity wave modes typically are taken to satisfy the synchronous gauge condition $\hat{t}^\mu h_{\mu\nu} = 0$ where \hat{t}^μ points along the time direction of the preferred coordinate system. In de Sitter space these conditions do not coincide for the flat and for the region I hyperbolic coordinatizations. These issues have been investigated for hyperbolic coordinates in flat Minkowski space.^[25]

In this paper we drop the approximation of no energy difference across the wall, which is never exactly the case in the presence of a bubble. This requires including finite critical bubble size as well. Taking these effects into account removes the infrared divergence of the CMB multipole moments. The calculation resembles the calculations for scalar perturbations in refs. [18, 21].

The organization of this paper as follows. Sections II and III give the multipole expansion for the pure tensor perturbations in hyperbolic space. Section II gives the evolution equation for the graviton field, which is solved by separation of variables. In section III we study the

[‡] We define *scalar*, *vector*, and *tensor* here such that a vector that can be expressed as the spatial gradient of a scalar is regarded as a *scalar*, a tensor that may be expressed as spatial derivatives acting on a *vector* is regarded as a *vector*, etc.

properties of tensor harmonics in three-dimensional hyperbolic space, first written down explicitly by Tomita [26]. As mentioned above, in section IV we identify the Bunch-Davies vacuum for the graviton field in region I in terms of the hyperbolic modes. In section V we compute the effect of nonvanishing bubble size and of nonvanishing energy density difference across the bubble wall. This result is used in section VI to give the tensor mode contribution to the CMB anisotropy for an open universe, and finally section VII concludes. There are two appendices containing technical details. We set $\hbar = 8\pi G = 1$ throughout, and $H = 1$ until section V.

2. Gravitational Waves in an Open Universe

Gravitational waves are fluctuations about a background metric. The metric can be written as a background metric $g_{\mu\nu}^B$ plus a small perturbation:

$$g_{\mu\nu} = g_{\mu\nu}^B + \hat{h}_{\mu\nu} \quad (2.1)$$

where we set $\hat{h}_{00} = 0$, $\hat{h}_{0i} = 0$, $\hat{h}_i{}^i = 0$, and $\hat{h}_{ij}{}^{||j} = 0$. These conditions require the *scalar* and *vector* perturbations to vanish and fix the gauge as well. The unperturbed spatial metric γ_{ij} (with line element $d\bar{s}^2 = d\xi^2 + \sinh^2[\xi]d\Omega_{(2)}^2$) is used to raise and lower roman indices, and the vertical line indicates the covariant derivative induced by γ_{ij} .

For the background corresponding to the natural coordinates in the interior of the bubble center's light cone, the background metric is given in eqn. (1.2). Hyperbolic conformal time

$$\eta = \ln \left[\tanh[t_h/2] \right], \quad (2.2)$$

will be used primarily in the following, in which the line element is

$$ds^2 = a^2[\eta] \cdot \left[-d\eta^2 + d\xi^2 + \sinh^2[\xi] d\Omega_{(2)}^2 \right], \quad (2.3)$$

where $-\infty < \eta < 0$.

The condition that the first order perturbation of the Ricci tensor vanishes $\delta R_{\mu\nu}^{(1)} = 0$ gives the equation of motion^[24]

$$g^{\alpha\beta} \nabla_\alpha \nabla_\beta \hat{h}_{\mu\nu} + 2R_{\alpha\mu\beta\nu}^{(B)} \hat{h}^{\alpha\beta} = 0. \quad (2.4)$$

This may be rewritten as

$$\left[D_\eta^2 - \nabla_{(3)}^2 + 2\mathcal{K} \right] h_{ij}(\xi, \theta, \phi, \eta) = 0, \quad (2.5)$$

where \mathcal{K} is the spatial curvature, with $\mathcal{K} = -1$ for a hyperbolic universe, and we have used $R_{ijkl}^{(B)} = \mathcal{K}(\gamma_{ik}\gamma_{jl} - \gamma_{jk}\gamma_{il})$. Using the ansatz

$$\mathcal{T}_i^j(\mathbf{x}, \eta; \zeta, P, j, m) = n(\zeta) \left[\mathbf{T}_{ij}^{P,jm}(\xi, \theta, \phi; \zeta) \right]_i^j T_h(\eta; \zeta), \quad (2.6)$$

we obtain

$$\begin{aligned} \left[\nabla_{(3)}^2 + (\zeta^2 + 3) \right] \mathbf{T}_{ij}^{P,jm}(\xi, \theta, \phi; \zeta) &= 0, \\ \left[\partial_\eta^2 + \frac{2a'}{a} \partial_\eta + (\zeta^2 + 1) \right] T_h(\eta; \zeta) &= 0. \end{aligned} \quad (2.7)$$

The normalization $n(\zeta)$ will be fixed later.

Using properties of the hyperbolic tensor harmonics that solve eqn. (2.7)a, the gravitational waves in region I can be expanded as[†]

$$\begin{aligned} \hat{h}_{rs}(\eta, \xi, \theta, \phi) &= \sum_{jmP} \int_0^\infty d\zeta n(\zeta) \mathbf{T}_{ij}^{P,jm}(\xi, \theta, \phi; \zeta) T_h(\eta; \zeta) \hat{a}_{P,j,m}(\zeta) + h.c. \\ &= \sum_{jmP} \int_0^\infty d\zeta \mathcal{T}_{ij}^{P,jm}(\xi, \theta, \phi, \eta; \zeta) \hat{a}_{P,j,m}(\zeta) + h.c. \end{aligned} \quad (2.8)$$

Here the operators $\hat{a}_I(\zeta, P, j, m)$, $a_I^\dagger(\zeta, P, j, m)$ satisfy the canonical commutation relations $[\hat{a}_I(\zeta, P, j, m), \hat{a}_I(\zeta', P', j', m')] = [\hat{a}_I^\dagger(\zeta, P, j, m), \hat{a}_I^\dagger(\zeta', P', j', m')] = 0$ and $[\hat{a}_I(\zeta, P, j, m), \hat{a}_I^\dagger(\zeta', P', j', m')] = \delta(\zeta - \zeta') \delta_{PP'} \delta_{jj'} \delta_{mm'}$ where $\zeta, \zeta' > 0$.

[†] It should be pointed out that in addition to the continuous modes with $0 \leq \zeta < \infty$ there might also exist some discrete *supercurvature* modes, as have been found for the minimally coupled scalar field in de Sitter space of mass m when $(m^2/H^2) < 2$. See refs. [14] and [27] for a discussion. The one supercurvature mode which would be expected to appear here by direct analogy has zero contribution to the CMB because of its lack of time dependence.

The spatial tensor harmonics and $n(\zeta)$ are discussed in the following section. Here the time dependence for the hyperbolic tensor modes and the flat tensor modes is found. For open de Sitter space, $a(\eta) = -1/\sinh[\eta]$. Thus for hyperbolic tensor modes eqn. (2.7)b becomes

$$T_h'' - 2 \coth[\eta] T_h' + (\zeta^2 + 1) T_h = 0, \quad (2.9)$$

replacing $-\nabla_{(3)}^2$ and \mathcal{K} with $(\zeta^2 + 3)$ and -1 , respectively. Transforming to the dependent variable $T = \sinh^2[\eta] \cdot F$, one may recast eqn. (2.9) into the form

$$F'' + 2 \coth[\eta] F' + (\zeta^2 + 1) F - \frac{2}{\sinh^2[\xi]} F = 0, \quad (2.10)$$

which is identical to the equation for the spatial hyperbolic radial functions with orbital angular momentum $l = 1$. [See for example ref. [10], eqn. (5.21).] It follows that

$$T_h(\eta; \zeta) = \{i\zeta \sinh[\eta] + \cosh[\eta]\} \cdot e^{-i\zeta\eta} \quad (2.11)$$

where ζ is allowed to take both signs.

For the flat tensor modes, which will be needed in order to find the Bunch-Davies vacuum, the time evolution equation becomes

$$T_f'' - \frac{2}{\bar{\eta}} T_f' + \omega^2 T_f = 0, \quad (2.12)$$

where we replace $-\nabla^2$ and \mathcal{K} with ω^2 and 0, respectively. With the substitution $T = \eta_f^{3/2} \cdot H$, eqn. (2.12) becomes the Bessel equation of order $\nu = 3/2$ whose solutions $H_{3/2}^{(+)}(\omega\eta_f)$ and $H_{3/2}^{(-)}(\omega\bar{\eta})$ are proportional to the spherical Bessel functions $h_1^{(+)}(\omega\eta_f)$ and $h_1^{(-)}(\omega\eta_f)$ multiplied by $\eta_f^{1/2}$. Consequently,

$$T_f(\eta_f; \omega) = \frac{1}{\omega^2} \cdot [1 + i\omega\eta_f] e^{-i\omega\eta_f} \quad (2.13)$$

where ω is allowed to take both signs.

3. Hyperbolic Tensor Harmonics

We now turn to computing and normalizing the hyperbolic tensor harmonics, which satisfy the equation

$$h_{ij}{}^{|k}{}_{|k} + (\zeta^2 + 3)h_{ij} = 0. \quad (3.1)$$

The offset in $(\zeta^2 + 3)$ is chosen for later convenience. The pure tensor character of these modes requires that they satisfy the conditions of tracelessness

$$h_i{}^i = 0, \quad (3.2)$$

and transversality

$$h_{ij}{}^{|j} = 0. \quad (3.3)$$

Here the roman letters $(i, j = 1, 2, 3)$ indicate spatial indices.

Since eqns. (3.1)–(3.3) are invariant under rotations and spatial inversion about $\xi = 0$, multipole solutions may be classified according to their angular momentum quantum numbers \mathbf{J}^2 , J_3 , and their parity π . Parity is either *electric* with $\pi = (-)^j$ or *magnetic* with $\pi = (-)^{j+1}$, denoted by $P = E$ and $P = M$, respectively. Fixing j , m , and P , we write down the most general symmetric tensor field with these quantum numbers. This restricts the angular dependence to a few terms but does not specify the radial dependence. Imposing eqns. (3.1)–(3.3) and solving for the ξ -dependence gives a solution for each $\zeta > 0$ and (j, m, P) for $j \geq 2$ unique up to an overall normalization. (There are no monopole ($j = 0$) or dipole ($j = 1$) modes.) The solution to these conditions has been found by Tomita[26].

The tensor field with electric parity has the form

$$\begin{aligned} \tilde{\mathbf{T}}^{E,jm}(\xi, \theta, \varphi; \zeta) = & F_j(\xi; \zeta) (\mathbf{e}^\xi \otimes \mathbf{e}^\xi) Y_{jm}(\theta, \varphi) \\ & + G_j(\xi; \zeta) \delta_{\tilde{a}\tilde{b}} (\mathbf{e}^{\tilde{a}} \otimes \mathbf{e}^{\tilde{b}}) Y_{jm}(\theta, \varphi) \\ & + H_j(\xi; \zeta) (\mathbf{e}^{\tilde{a}} \otimes \mathbf{e}^\xi + \mathbf{e}^\xi \otimes \mathbf{e}^{\tilde{a}}) \tilde{\nabla}_{\tilde{a}} Y_{jm}(\theta, \varphi) \\ & + I_j(\xi; \zeta) (\mathbf{e}^{\tilde{a}} \otimes \mathbf{e}^{\tilde{b}}) \tilde{\nabla}_{\tilde{a}} \tilde{\nabla}_{\tilde{b}} Y_{jm}(\theta, \varphi) \end{aligned} \quad (3.4)$$

where $(\tilde{a}, \tilde{b} = 1, 2)$ indicate angular indices and $\tilde{\nabla}$ indicates an S^2 (rather than an H^3)

covariant derivative. As a result, $\delta_{\tilde{a}\tilde{b}} (\mathbf{e}^{\tilde{a}} \otimes \mathbf{e}^{\tilde{b}}) = (\mathbf{e}^\theta \otimes \mathbf{e}^\theta + \sin^2 \theta \mathbf{e}^\varphi \otimes \mathbf{e}^\varphi)$. The basis functions are $\mathbf{e}^\xi = d\xi$, $\mathbf{e}^\theta = d\theta$, and $\mathbf{e}^\varphi = d\varphi$. Note that this is not a *vielbein* (normalized) basis.

We use

$$\nabla^2 = D_\xi^2 + 2 \coth[\xi] D_\xi + \frac{1}{\sinh^2[\xi]} \cdot \left[D_\theta^2 + \cot[\theta] D_\theta + \frac{1}{\sin^2 \theta} D_\varphi^2 \right] \quad (3.5)$$

and

$$\begin{aligned} D_\xi \mathbf{e}^\xi &= 0, & D_\theta \mathbf{e}^\varphi &= -\cot[\theta] \mathbf{e}^\varphi, \\ D_\xi \mathbf{e}^\theta &= -\coth[\xi] \mathbf{e}^\theta, & D_\varphi \mathbf{e}^\xi &= +\sinh[\xi] \cosh[\xi] \sin^2[\theta] \mathbf{e}^\theta, \\ D_\xi \mathbf{e}^\varphi &= -\coth[\xi] \mathbf{e}^\varphi, & D_\varphi \mathbf{e}^\theta &= +\sin[\theta] \cos \theta \mathbf{e}^\varphi, \\ D_\theta \mathbf{e}^\xi &= +\sinh[\xi] \cosh[\xi] \mathbf{e}^\theta, & D_\varphi \mathbf{e}^\varphi &= -\cot[\theta] \mathbf{e}^\theta - \coth[\xi] \mathbf{e}^\xi, \\ D_\theta \mathbf{e}^\theta &= -\coth[\xi] \mathbf{e}^\xi. \end{aligned} \quad (3.6)$$

We now impose the constraints of transversality and tracelessness. For transversality, taking the divergence of $\mathbf{T}^{jm,E}$ gives

$$\begin{aligned} \nabla \cdot T_{jm} &= \left[\frac{\partial F}{\partial \xi} + 2 \coth[\xi] F(\xi) - \frac{2 \coth[\xi]}{\sinh^2[\xi]} G(\xi) - \frac{j(j+1)}{\sinh^2[\xi]} H(\xi) \right. \\ &\quad \left. + \frac{j(j+1) \coth[\xi]}{\sinh^2[\xi]} I(\xi) \right] Y_{jm}(\Omega) \times \mathbf{e}^\xi \\ &\quad + \left[\frac{G(\xi)}{\sinh^2[\xi]} + \frac{\partial H}{\partial \xi} + 2 \coth[\xi] H(\xi) - \frac{1}{\sinh^2[\xi]} \cdot [j(j+1) - 1] I(\xi) \right] \\ &\quad \times \left[\mathbf{e}^\theta \frac{\partial Y_{jm}}{\partial \theta} + \mathbf{e}^\varphi \frac{\partial Y_{jm}}{\partial \varphi} \right] = 0. \end{aligned} \quad (3.7)$$

Both terms must individually vanish. Likewise, taking the trace and asking it to vanish gives the condition

$$T_i^i = F(\xi) + \frac{2G(\xi)}{\sinh^2[\xi]} - \frac{j(j+1)I(\xi)}{\sinh^2[\xi]} = 0. \quad (3.8)$$

Thus transversality and tracelessness give

$$\begin{aligned}
H_j(\xi; \zeta) &= \frac{\sinh^2[\xi]}{j(j+1)} \cdot \left[\frac{\partial F_j(\xi; \zeta)}{\partial \xi} + 3 \coth[\xi] F_j(\xi; \zeta) \right], \\
I_j(\xi; \zeta) &= \frac{\sinh^2[\xi]}{(j+2)(j-1)} \cdot \left[2 \left(\frac{\partial H_j(\xi; \zeta)}{\partial \xi} + 2 \coth[\xi] H_j(\xi; \zeta) \right) - F_j(\xi; \zeta) \right], \\
G_j(\xi; \zeta) &= \frac{1}{2} \left[j(j+1) I_j(\xi; \zeta) - \sinh^2[\xi] F_j(\xi; \zeta) \right].
\end{aligned} \tag{3.9}$$

The Laplacian in eqn. (3.5) acting on the various components of $\tilde{\mathbf{T}}^{E,jm}$ in eqn. (3.4) gives

$$\begin{aligned}
&\nabla^2 \left[F(\xi) Y_{jm}(\Omega) \cdot (\mathbf{e}^\xi \otimes \mathbf{e}^\xi) \right] \\
&= \left[\frac{\partial^2 F}{\partial \xi^2} + 2 \coth[\xi] \frac{\partial F}{\partial \xi} - \left(\frac{j(j+1)}{\sinh^2[\xi]} + 4 \coth^2[\xi] \right) F(\xi) \right] Y_{jm}(\Omega) \cdot (\mathbf{e}^\xi \otimes \mathbf{e}^\xi) \\
&+ [2 \cosh^2[\xi] F(\xi) Y_{jm}(\Omega)] \cdot (\mathbf{e}^\theta \otimes \mathbf{e}^\theta + \sin^2 \theta \mathbf{e}^\varphi \otimes \mathbf{e}^\varphi) \\
&+ [2 \coth[\xi] F(\xi)] \cdot \left[(\mathbf{e}^\xi \otimes \mathbf{e}^\theta + \mathbf{e}^\theta \otimes \mathbf{e}^\xi) \frac{\partial Y_{jm}}{\partial \theta} + (\mathbf{e}^\xi \otimes \mathbf{e}^\varphi + \mathbf{e}^\varphi \otimes \mathbf{e}^\xi) \frac{\partial Y_{jm}}{\partial \varphi} \right],
\end{aligned} \tag{3.10}$$

$$\begin{aligned}
&\nabla^2 \left[G(\xi) Y_{jm}(\Omega) \cdot (\mathbf{e}^\theta \otimes \mathbf{e}^\theta + \sin^2 \theta \mathbf{e}^\varphi \otimes \mathbf{e}^\varphi) \right] \\
&= \left[\frac{4 \coth^2[\xi]}{\sinh^2[\xi]} G(\xi) Y_{jm}(\Omega) \right] \cdot (\mathbf{e}^\xi \otimes \mathbf{e}^\xi) \\
&+ \left[\frac{\partial^2 G}{\partial \xi^2} - 2 \coth[\xi] \frac{\partial G}{\partial \xi} - 2G - \frac{j(j+1)}{\sinh^2[\xi]} G \right] Y_{jm}(\Omega) \cdot (\mathbf{e}^\theta \otimes \mathbf{e}^\theta + \sin^2 \theta \mathbf{e}^\varphi \otimes \mathbf{e}^\varphi) \\
&- \frac{2 \cosh[\xi]}{\sinh^3[\xi]} G(\xi) \cdot \left[(\mathbf{e}^\xi \otimes \mathbf{e}^\theta + \mathbf{e}^\theta \otimes \mathbf{e}^\xi) \frac{\partial Y_{jm}}{\partial \theta} + (\mathbf{e}^\xi \otimes \mathbf{e}^\varphi + \mathbf{e}^\varphi \otimes \mathbf{e}^\xi) \frac{\partial Y_{jm}}{\partial \varphi} \right],
\end{aligned} \tag{3.11}$$

$$\begin{aligned}
& \nabla^2 \left[H(\xi) \cdot \left\{ (\mathbf{e}^\xi \otimes \mathbf{e}^\theta + \mathbf{e}^\theta \otimes \mathbf{e}^\xi) \frac{\partial Y_{jm}}{\partial \theta} + (\mathbf{e}^\xi \otimes \mathbf{e}^\varphi + \mathbf{e}^\varphi \otimes \mathbf{e}^\xi) \frac{\partial Y_{jm}}{\partial \varphi} \right\} \right] \\
&= \frac{4j(j+1) \coth[\xi]}{\sinh^2[\xi]} Y_{jm}(\Omega) H(\xi) \cdot (\mathbf{e}^\xi \otimes \mathbf{e}^\xi) \\
&+ \left[\frac{\partial^2 H}{\partial \xi^2} - 2H - 4 \coth^2[\xi] H - \frac{j(j+1)}{\sinh^2[\xi]} H \right] \\
&\times \left[(\mathbf{e}^\xi \otimes \mathbf{e}^\theta + \mathbf{e}^\theta \otimes \mathbf{e}^\xi) \frac{\partial Y_{jm}}{\partial \theta} + (\mathbf{e}^\xi \otimes \mathbf{e}^\varphi + \mathbf{e}^\varphi \otimes \mathbf{e}^\xi) \frac{\partial Y_{jm}}{\partial \varphi} \right] \\
&+ 4H(\xi) \coth[\xi] \cdot \left[(\mathbf{e}^\theta \otimes \mathbf{e}^\theta) \frac{\partial^2 Y_{jm}}{\partial \theta^2} + (\mathbf{e}^\varphi \otimes \mathbf{e}^\varphi) \left(\frac{\partial^2 Y_{jm}}{\partial \varphi^2} + \sin \theta \cos \theta \frac{\partial Y_{jm}}{\partial \theta} \right) \right. \\
&\quad \left. + (\mathbf{e}^\theta \otimes \mathbf{e}^\varphi + \mathbf{e}^\varphi \otimes \mathbf{e}^\theta) \left(\frac{\partial^2 Y_{jm}}{\partial \theta \partial \varphi} - \cot \theta \frac{\partial Y_{jm}}{\partial \varphi} \right) \right], \tag{3.12}
\end{aligned}$$

and

$$\begin{aligned}
& \nabla^2 \left[I(\xi) \left\{ (\mathbf{e}^\theta \otimes \mathbf{e}^\theta) \frac{\partial^2 Y_{jm}}{\partial \theta^2} + (\mathbf{e}^\varphi \otimes \mathbf{e}^\varphi) \left(\frac{\partial^2 Y_{jm}}{\partial \varphi^2} + \sin \theta \cos \theta \frac{\partial Y_{jm}}{\partial \theta} \right) \right. \right. \\
&\quad \left. \left. + (\mathbf{e}^\theta \otimes \mathbf{e}^\varphi + \mathbf{e}^\varphi \otimes \mathbf{e}^\theta) \left(\frac{\partial^2 Y_{jm}}{\partial \theta \partial \varphi} - \cot \theta \frac{\partial Y_{jm}}{\partial \varphi} \right) \right\} \right] \\
&= \frac{-2I(\xi)j(j+1) \coth^2[\xi]}{\sinh^2[\xi]} Y_{jm}(\Omega) \cdot (\mathbf{e}^\xi \otimes \mathbf{e}^\xi) \\
&+ \frac{2I(\xi)j(j+1)}{\sinh^2[\xi]} Y_{jm}(\Omega) \cdot (\mathbf{e}^\theta \otimes \mathbf{e}^\theta + \sin^2 \theta \mathbf{e}^\varphi \otimes \mathbf{e}^\varphi) \\
&+ \frac{2[j(j+1) - 1] \coth[\xi] I(\xi)}{\sinh^2[\xi]} \\
&\times (\mathbf{e}^\xi \otimes \mathbf{e}^\theta + \mathbf{e}^\theta \otimes \mathbf{e}^\xi) \frac{\partial Y_{jm}}{\partial \theta} + (\mathbf{e}^\xi \otimes \mathbf{e}^\varphi + \mathbf{e}^\varphi \otimes \mathbf{e}^\xi) \frac{\partial Y_{jm}}{\partial \varphi} \\
&+ \left[\frac{\partial^2 I}{\partial \xi^2} - 2 \coth[\xi] \frac{\partial}{\partial \xi} + \frac{6I(\xi)}{\sinh^2[\xi]} - 2I(\xi) \coth^2[\xi] - \frac{j(j+1)}{\sinh^2[\xi]} I(\xi) \right] \\
&\times \left[(\mathbf{e}^\theta \otimes \mathbf{e}^\theta) \frac{\partial^2 Y_{jm}}{\partial \theta^2} + (\mathbf{e}^\varphi \otimes \mathbf{e}^\varphi) \left(\frac{\partial^2 Y_{jm}}{\partial \varphi^2} + \sin \theta \cos \theta \frac{\partial Y_{jm}}{\partial \theta} \right) \right. \\
&\quad \left. + (\mathbf{e}^\theta \otimes \mathbf{e}^\varphi + \mathbf{e}^\varphi \otimes \mathbf{e}^\theta) \left(\frac{\partial^2 Y_{jm}}{\partial \theta \partial \varphi} - \cot \theta \frac{\partial Y_{jm}}{\partial \varphi} \right) \right]. \tag{3.13}
\end{aligned}$$

To solve for $F_j(\xi; \zeta)$, we take the $(\mathbf{e}^\xi \otimes \mathbf{e}^\xi)$ component of the Laplacian acting on eqn. (3.4), and after applying the substitutions in eqn. (3.9), the coefficient of $\mathbf{e}^\xi \otimes \mathbf{e}^\xi$ term in (3.1) be-

comes

$$\frac{\partial^2 F_j(\xi; \zeta)}{\partial \xi^2} + 6 \coth[\xi] \frac{\partial F_j(\xi; \zeta)}{\partial \xi} + \left[(\zeta^2 + 3) + 6 \coth^2[\xi] - \frac{j(j+1)}{\sinh^2[\xi]} \right] F_j(\xi; \zeta) = 0. \quad (3.14)$$

With the change of variable $\phi_j(\xi; \zeta) = \sinh^2[\xi] \cdot F_j(\xi; \zeta)$, one recovers the differential equation for the *scalar* hyperbolic radial functions (see, for example, [10] eqn. (5.21)):

$$\frac{\partial^2 \phi_j(\xi; \zeta)}{\partial \xi^2} + 2 \coth[\xi] \frac{\partial \phi_j(\xi; \zeta)}{\partial \xi} + \left[(\zeta^2 + 1) - \frac{j(j+1)}{\sinh^2[\xi]} \right] \phi_j(\xi; \zeta) = 0. \quad (3.15)$$

Consequently,

$$F_j(\xi; \zeta) = N_j(\zeta) \cdot \sinh^{j-2}[\xi] \frac{d^{j+1}}{d(\cosh[\xi])^{j+1}} \cos[\zeta \xi] \quad (3.16)$$

where the normalization $N_j(\zeta)$ is determined in the following, and we have imposed regularity at the origin.

For future reference, for $j = 2$

$$F_2(\xi; \zeta) = \frac{N_2(\zeta)}{\sinh^3[\xi]} \cdot \left[3\zeta^2 \coth[\xi] \cos[\zeta \xi] + (\zeta^3 + \zeta - 3\zeta \coth^2[\xi]) \sin[\zeta \xi] \right]. \quad (3.17)$$

and from eqn. (3.9)

$$\begin{aligned} G_2(\xi; \zeta) &= N_2(\zeta) \cdot \sinh[\xi] \cdot \left[\left\{ \frac{\zeta^2 \coth[\xi]}{4} (1 - 2\zeta^2 - 3 \coth^2[\xi]) \right\} \sin[\zeta \xi] \right. \\ &\quad \left. + \left\{ \frac{-\zeta^5 - 2\zeta^3 - \zeta}{4} + \frac{\zeta \coth^2[\xi]}{4} (\zeta^2 - 2 + 3 \coth^2[\xi]) \right\} \cos[\zeta \xi] \right], \\ H_2(\xi; \zeta) &= N_2(\zeta) \cdot \frac{1}{\sinh[\xi]} \cdot \left[\left\{ \frac{\zeta^2}{6} (\zeta^2 + 4 - 6 \coth^2[\xi]) \right\} \cos[\zeta \xi] \right. \\ &\quad \left. + \left\{ \frac{\zeta \coth[\xi]}{2} (2 \coth^2[\xi] - \zeta^2 - 2) \right\} \sin[\zeta \xi] \right], \\ I_2(\xi; \zeta) &= N_2(\zeta) \cdot \sinh[\xi] \cdot \left[\left\{ \frac{\zeta^2 \coth[\xi]}{12} (-5 - 2\zeta^2 + 3 \coth^2[\xi]) \right\} \cos[\zeta \xi] \right. \\ &\quad \left. + \left\{ \frac{-\zeta^5 - 4\zeta^3 - 3\zeta}{12} + \frac{\zeta \coth^2[\xi]}{4} (-\coth^2[\xi] + \zeta^2 + 2) \right\} \sin[\zeta \xi] \right]. \end{aligned} \quad (3.18)$$

Similarly, for the magnetic parity, the tensor field must take the form

$$\begin{aligned} \mathbf{T}^{B,jm}(\xi, \theta, \varphi; \zeta) = & U(\xi; \zeta) (\mathbf{e}^{\tilde{a}} \otimes \mathbf{e}^\xi + \mathbf{e}^\xi \otimes \mathbf{e}^{\tilde{a}}) \mathbf{L}_{\tilde{a}} Y_{jm}(\theta, \varphi) \\ & + V(\xi; \zeta) (\mathbf{e}^{\tilde{a}} \otimes \mathbf{e}^{\tilde{b}} + \mathbf{e}^{\tilde{b}} \otimes \mathbf{e}^{\tilde{a}}) \mathbf{L}_{\tilde{a}} \tilde{\nabla}_{\tilde{b}} Y_{jm}(\theta, \varphi). \end{aligned} \quad (3.19)$$

The magnetic parity modes do not contribute to the CMB anisotropy because their component along the $(\mathbf{e}^\xi \otimes \mathbf{e}^\xi)$ direction vanishes; therefore, we do not give their explicit form.

Normalization of the Hyperbolic Tensor Harmonics. To normalize the tensor harmonics, we impose the condition

$$\begin{aligned} \int_0^\infty d\xi \int d\Omega \sqrt{\hat{g}_{(3)}} T_{ij}(\mathbf{x}; \zeta, P, j, m)^* T^{ij}(\mathbf{x}; \zeta', P', j', m') \\ = \delta(\zeta - \zeta') \cdot \delta_{P,P'} \cdot \delta_{j,j'} \cdot \delta_{m,m'} \end{aligned} \quad (3.20)$$

where P indicates mode parity and $\mathbf{x} = (\xi, \theta, \phi)$.

Because the tensor harmonics are eigenfunctions of a self-adjoint operator, the inner product is proportional to a δ -function. Thus $N_j(\zeta)$ is determined by the coefficients of $e^{\pm i\zeta\xi}$ in the asymptotic expansion of the tensor harmonics for large ξ . (For $\xi \rightarrow 0$, $F_j, H_j, G_j, I_j \rightarrow 0$.) In comparing the asymptotic behaviors of F, G, H and I , it is more meaningful to consider the rescaled quantities $\hat{F}_j(\xi; \zeta) = F_j(\xi; \zeta)$, $\hat{G}_j(\xi; \zeta) = G_j(\xi; \zeta)/\sinh^2[\xi]$, $\hat{H}_j(\xi; \zeta) = H_j(\xi; \zeta)/\sinh[\xi]$, and $\hat{I}_j(\xi; \zeta) = I_j(\xi; \zeta)/\sinh^2[\xi]$, components with respect to a normalized ‘vielbein’ basis. From eqn. (3.9), $\hat{F} \sim \sinh^{-3}[\xi]$, $\hat{H} \sim \sinh^{-2}[\xi]$, and $\hat{G}, \hat{I} \sim \sinh^{-1}[\xi]$. For $\xi \gg \lambda$, \hat{G} and \hat{I} dominate, exactly as one would expect. That is, at large distances a spherical gravitational wave should locally resemble a plane gravitational wave propagating in the radial direction.

To compute the coefficient of the δ -function in eqn. (3.20), we impose a boundary condition at $\xi = \xi_{max}$ (for specificity say Dirichlet boundary conditions) and take the limit $\xi_{max} \rightarrow \infty$. For $\xi_{max} \gg 1$, the integral in eqn. (3.20) is dominated by the G and I components. These may be approximated by their large- ξ asymptotic forms, starting with

eqn. (3.16) and substituting $\sinh[\xi] \rightarrow (e^\xi/2) = (w/2)$. This gives

$$\begin{aligned} F_j(\xi; \zeta) &\approx 4 N_j(\zeta) w^{-3} \left(\frac{d}{dw} \right)^{j+1} [w^{+i\zeta} + w^{-i\zeta}] \\ &= 4 N_j(\zeta) e^{-3\xi} \cdot \left[(i\zeta)_j e^{+i\zeta\xi} + c.c. \right]. \end{aligned} \quad (3.21)$$

Here $(x)_j$ is shorthand for $x(x-1)\dots(x-j)$. Using eqn. (3.9), we obtain

$$\begin{aligned} H_j(\xi; \zeta) &\approx \frac{4 N_j(\zeta) e^{-\xi}}{j(j+1)} \cdot \left[(i\zeta) \cdot (i\zeta)_j e^{+i\zeta\xi} + c.c. \right], \\ I_j(\xi; \zeta) &\approx \frac{2 N_j(\zeta) e^{+\xi}}{j(j+1)(j-1)(j+2)} \cdot \left[(i\zeta+1) \cdot (i\zeta) \cdot (i\zeta)_j e^{+i\zeta\xi} + c.c. \right], \\ G_j(\xi; \zeta) &\approx \frac{N_j(\zeta) e^{+\xi}}{(j-1)(j+2)} \cdot \left[(i\zeta+1) \cdot (i\zeta) \cdot (i\zeta)_j e^{+i\zeta\xi} + c.c. \right]. \end{aligned} \quad (3.22)$$

Consequently, for $(\xi \gg 1)$,

$$\begin{aligned} \mathbf{T}(\mathbf{x}; \zeta, E, j, m) &\approx \left[\frac{2N_j(\zeta)e^\xi}{j(j+1)(j-1)(j+2)} \cdot (i\zeta+1) \cdot (i\zeta) \cdot (i\zeta)_j \cdot e^{+i\zeta\xi} \right. \\ &\quad \times \left. \left[\nabla_{\tilde{a}} \nabla_{\tilde{b}} Y_{jm}(\theta, \phi) + \delta_{\tilde{a}\tilde{b}} \frac{1}{2} j(j+1) Y_{jm}(\theta, \phi) \right] \left(\hat{\mathbf{e}}^{\tilde{a}} \otimes \hat{\mathbf{e}}^{\tilde{b}} \right) \right] \\ &\quad + c.c. \end{aligned} \quad (3.23)$$

Inserting this asymptotic expression into eqn. (3.20) and factoring out $\delta_{jj'} \delta_{mm'}$ gives

$$\begin{aligned} &\int_0^{\xi_{max}} d\xi \sinh^2[\xi] \int d\Omega T_{ij}(\mathbf{x}; \zeta, E, j, m) T^{ij}(\mathbf{x}; \zeta, E, j, m)^* \\ &\approx |N_j(\zeta)|^2 \cdot \frac{4\zeta^2(\zeta^2+1) [\zeta^2(\zeta^2+1^2) \dots (\zeta^2+j^2)]}{j^2(j+1)^2(j-1)^2(j+2)^2} \\ &\quad \times \frac{\xi_{max}}{2} \int d\Omega \left| \nabla_{\tilde{a}} \nabla_{\tilde{b}} Y_{jm} + \frac{1}{2} \delta_{\tilde{a}\tilde{b}} j(j+1) Y_{jm} \right|^2. \end{aligned} \quad (3.24)$$

For the angular integration, note that

$$\begin{aligned}
\int d\Omega \left(\nabla_{\tilde{a}} \nabla_{\tilde{b}} Y_{jm} \right)^* \nabla^{\tilde{a}} \nabla^{\tilde{b}} Y_{jm} &= - \int d\Omega \left(\nabla^{\tilde{a}} \nabla_{\tilde{a}} \nabla_{\tilde{b}} Y_{jm} \right)^* \left(\nabla^{\tilde{b}} Y_{jm} \right) \\
&= - \int d\Omega \left(\nabla_{\tilde{a}} \nabla_{\tilde{b}} \nabla^{\tilde{a}} Y_{jm} \right)^* \left(\nabla^{\tilde{b}} Y_{jm} \right) \\
&= - \int d\Omega \left(\nabla_{\tilde{b}} \left\{ \nabla^2 + \frac{1}{2} R \right\} Y_{jm} \right)^* \left(\nabla^{\tilde{b}} Y_{jm} \right) \\
&= [j(j+1)] \cdot [j(j+1) - 1],
\end{aligned} \tag{3.25}$$

given that $g^{\tilde{a}\tilde{c}} [\nabla_{\tilde{a}}, \nabla_{\tilde{b}}] \nabla_{\tilde{c}} f = g^{\tilde{a}\tilde{c}} R_{\tilde{a}\tilde{b}\tilde{c}} \tilde{d} \nabla_{\tilde{d}} f = R_{\tilde{b}}^{\tilde{d}} (\nabla_{\tilde{d}} f) = \frac{1}{2} R \nabla_{\tilde{b}} f$. Since the unit two-sphere is isotropic, $R_{\tilde{a}\tilde{b}} = \frac{1}{2} \delta_{\tilde{a}\tilde{b}} R$. Also, for the two-sphere $R = 2$. Thus the integral on the last line of eqn. (3.24) is equal to $[j(j+1)][\frac{1}{2}j(j+1) - 1]$, and eqn. (3.24) reduces to

$$|N_j(\zeta)|^2 \cdot \frac{4[j(j+1)][\frac{1}{2}j(j+1) - 1]}{j^2(j+1)^2(j-1)^2(j+2)^2} \times \zeta^2(\zeta^2 + 1)[\zeta^2(\zeta^2 + 1^2) \dots (\zeta^2 + j^2)] \times \frac{\xi_{max}}{2}, \tag{3.26}$$

from which it follows that

$$N_j(\zeta) = \frac{1}{\sqrt{\pi}} \frac{\sqrt{j(j+1)(j-1)(j+2)}}{\zeta \sqrt{1 + \zeta^2} \sqrt{\zeta^2(\zeta^2 + 1^2) \dots (\zeta^2 + j^2)}}. \tag{3.27}$$

The $\pi^{-1/2}$ comes from passing to the continuum and the phase of $N_j(\zeta)$ has been chosen to be real.

Flat Tensor Harmonics. The general form of the flat modes is needed to identify the Bunch-Davies vacuum in the next section. These may be regarded as the large- ζ , small- ξ limit of the hyperbolic modes, a limit in which the effects of spatial curvature disappear. We use lower case letters to denote the flat analogues of hyperbolic quantities. In particular,

$$f(r, \omega) = \bar{n}_j(\omega) \cdot r^{j-2} \left(\frac{1}{r} \frac{d}{dr} \right)^{j+1} \cos[\omega r]. \tag{3.28}$$

Similarly, eqn. (3.9) is modified to

$$\begin{aligned}
h_j(r; \omega) &= \frac{r^2}{j(j+1)} \left[\frac{\partial f_j}{\partial r} + \frac{3}{r} f_j \right], \\
i_j(r; \omega) &= \frac{r^2}{(j+2)(j-1)} \left[2 \frac{\partial h_j}{\partial r} + \frac{4}{r} h_j - f_j \right], \\
g_j(r; \omega) &= \frac{1}{2} [j(j+1) i_j(r) - r^2 f_j].
\end{aligned} \tag{3.29}$$

In particular, for $j = 2$

$$\begin{aligned}
f_2(r; \omega) &= \left(\frac{3\omega^2}{r^3} \right) \cos[\omega r] + \left(\frac{-3\omega}{r^4} + \frac{\omega^3}{r^2} \right) \sin[\omega r], \\
g_2(r; \omega) &= \left(\frac{-3\omega^2}{r} \right) \cos[\omega r] + \left(\frac{-\omega^5 r^2}{4} - \omega^3 + \frac{3\omega}{r^2} \right) \sin[\omega r], \\
h_2(r; \omega) &= \left(\frac{-\omega^2}{2r^2} + \frac{\omega^4}{6} \right) \cos[\omega r] + \left(\frac{-\omega^3}{3r} + \frac{\omega}{2r^3} \right) \sin[\omega r], \\
i_2(r; \omega) &= \left(\frac{-\omega^2}{2r} \right) \cos[\omega r] + \left(\frac{-\omega^5 r^2}{12} - \frac{\omega^3}{6} + \frac{\omega}{2r^2} \right) \sin[\omega r].
\end{aligned} \tag{3.30}$$

In order to calculate the normalization, one needs the asymptotic behavior for large r :

$$\begin{aligned}
f_j(\xi; \omega) &\approx \bar{n}_j(\zeta) \cdot \frac{1}{2r^3} \left[(i\omega)^{j+1} e^{+i\omega r} + c.c. \right], \\
h_j(\xi; \omega) &\approx \bar{n}_j(\zeta) \cdot \frac{1}{j(j+1)} \cdot \frac{1}{2r} \left[(i\omega)^{j+2} e^{+i\omega r} + c.c. \right], \\
i_j(\xi; \omega) &\approx \bar{n}_j(\zeta) \cdot \frac{1}{j(j+1)(j-1)(j+2)} \cdot r \cdot \left[(i\omega)^{j+3} e^{+i\omega r} + c.c. \right], \\
g_j(\xi; \omega) &\approx \bar{n}_j(\zeta) \cdot \frac{1}{2(j-1)(j+2)} \cdot r \cdot \left[(i\omega)^{j+3} e^{+i\omega r} + c.c. \right].
\end{aligned} \tag{3.31}$$

Again i_j and g_j dominate, and following the same steps as for the hyperbolic modes we get

$$\bar{n}_j(\omega) = \frac{\sqrt{j(j+1)(j+2)(j-1)}}{\sqrt{\pi}\omega^{j+3}}. \tag{3.32}$$

This is the $\zeta \rightarrow \omega \gg j$ limit of eqn. (3.27).

Normalization of the Time Dependent Mode Functions. We may define the anti-symmetric bilinear form

$$\langle \mathcal{U}, \mathcal{V} \rangle = - \int_{\Sigma} d\Sigma^\mu \mathcal{U}_{\alpha\beta}(\Sigma) (i\overleftrightarrow{D}_\mu) \mathcal{V}^{\alpha\beta}(\Sigma), \tag{3.33}$$

where \mathcal{U}, \mathcal{V} are solutions to eqn. (2.4). This product is analogous to the Klein-Gordon product for scalar field modes. Eqn. (2.4) insures that the current $\mathcal{U}_{AB}(\Sigma) (i\overleftrightarrow{\nabla}_\mu) \mathcal{V}^{AB}(\Sigma)$

is conserved and thus that $\langle \mathcal{U}, \mathcal{V} \rangle$ is invariant under deformations of the surface Σ . In order that the modes for a spacetime M orthonormalized with respect to (3.33) are associated with operators that satisfy the customary canonical commutation relations, it is necessary to choose Σ in (3.33) so that Σ is a Cauchy surface for M . The product $\langle \cdot, \cdot \rangle$ is the same for all Cauchy surfaces for the spacetime M . A Cauchy surface is a spacelike hypersurface which each non-spacelike curve intersects once and only once [28]. In this paper we shall consider both the case where M is just region I, in which case a surface of constant region I hyperbolic time serves as a convenient choice of Cauchy surface, and also the case where M is all of maximally extended de Sitter space, in which case the surface defined by $\tau = 0$ in the region II hyperbolic coordinates serves as a convenient Cauchy surface.

For the hyperbolic modes defined in eqn. (2.6) in region I one calculates

$$\begin{aligned}
& \langle \mathcal{T}(\zeta, P, j, m), \mathcal{T}(\zeta', P', j', m')^* \rangle \\
&= - \int_{\Sigma} d^3x a^3(\eta) \left[\mathcal{T}_{\alpha}^{\beta}(\mathbf{x}, \eta; \zeta, P, j, m) (i \overleftrightarrow{D}_{\hat{0}}) \mathcal{T}_{\beta}^{\alpha}(\mathbf{x}, \eta; \zeta', P', j', m')^* \right] \\
&= n^2(\zeta) 2 \zeta (\zeta^2 + 1) \cdot \delta(\zeta - \zeta') \cdot \delta_{P, P'} \cdot \delta_{j, j'} \cdot \delta_{m, m'}
\end{aligned} \tag{3.34}$$

where $D_{\hat{0}} = (1/a)D_{\eta} = -\sinh[\eta]D_{\eta}$. Note that eqn. (3.34) is independent of η . This may be seen by applying D_{η} to eqn. (3.34) and using eqn. (2.9). For the mixed tensor representation chosen above, the covariant derivative $D_{\hat{0}}$ may be replaced with the ordinary derivative $\partial_{\hat{0}}$. So, reading off,

$$n(\zeta) = \frac{1}{\sqrt{2\zeta(\zeta^2 + 1)}}. \tag{3.35}$$

As the initial conditions are determined by the bubble which extends outside of region I, a proper Cauchy surface for initial conditions for an open universe extends outside of region I as well. It was shown in [14] that for some cases, inner products taken on a Cauchy surface in region II agreed with those on fixed time surfaces in region I and V, even though the latter do not make up a Cauchy surface for the whole spacetime. The norms agreed for scalar fields with sufficiently fast falloff at infinity, a condition satisfied by subcurvature modes of the Laplacian (modes with eigenvalue $\zeta^2 + 1 \geq 1$). There are some differences in extending this comparison between norms taken in I and V and norms taken in II for

gravity waves. When the gravity waves are continued across the light cone, into region II, time and space are interchanged and the gauge choice becomes $h_{u\mu} = 0$ instead of $h_{\eta\mu} = 0$. As u is a spacelike coordinate, this is not the usual gauge for metric perturbations. It may be thought of as analogous to axial gauge (where $A_3 = 0$) rather than Coulomb gauge (where $A_0 = 0$) in electrodynamics. Secondly, the inner product in region II involves a wronskian in (the analytic continuation of) ξ , and is more complicated due to the tensor structure in ξ . As shown in appendix B, this inner product on a Cauchy surface in region II coincides with the inner product in regions I, V, for modes which have sufficiently fast falloff at infinity. The fields with sufficiently fast falloff for gravity waves are again subcurvature modes, $0 \leq \zeta^2 < \infty$. As the falloff for the gravity wave modes is as fast as that for the scalars in regions I, V (both go as $\sinh^{-1}[\xi]$ for large ξ), it was reasonable to expect this.

4. Identifying the Gravitational Wave Bunch-Davies Vacuum

The preceding section gave the mode expansion for the linearized gravitational waves in region I hyperbolic coordinates, which are the natural coordinates for the open universe inside the bubble. In this section the initial Bunch-Davies vacuum is expressed in terms of these open hyperbolic modes. In the open universe inflationary scenario, the Bunch-Davies vacuum is a preferred quantum state for de Sitter space in the sense that it is a weak attractor: any initial quantum state for perturbations from de Sitter space, subject only to the requirement that the initial energy density be finite, approaches the Bunch-Davies vacuum to arbitrary accuracy after a sufficient amount of inflationary expansion. The convergence is weak rather than strong because the initial perturbations are not erased but rather pushed to larger and larger scales, so that for an observer able to probe only a fixed physical volume, the perturbations seem to disappear.

The Bunch-Davies vacuum is physically characterized using the flat coordinates for de Sitter space. In these coordinates, at sufficiently early times, a mode of fixed co-moving wavenumber evolves as if it were a mode in Minkowski space. For the flat coordinates the line element is

$$ds^2 = -dt_f^2 + e^{2t_f} \cdot \left[dr_f^2 + r_f^2 d\Omega_{(2)}^2 \right] \quad (4.1)$$

where $-\infty < t_f < +\infty$, or in terms of flat conformal time $\eta_f = -e^{-t_f}$

$$ds^2 = \frac{1}{\eta_f^2} \cdot \left[-d\eta_f^2 + dr_f^2 + r_f^2 d\Omega_{(2)}^2 \right]. \quad (4.2)$$

Early on, when the mode is subhorizon, so that there are many oscillations within an expansion time, one identifies the mode with positive frequency asymptotic behavior with an annihilation operator of the Bunch-Davies vacuum. These are the modes that behave as $e^{-ik\eta_f}/\eta_f$ for $\eta_f \rightarrow -\infty$, where η_f is flat conformal time.

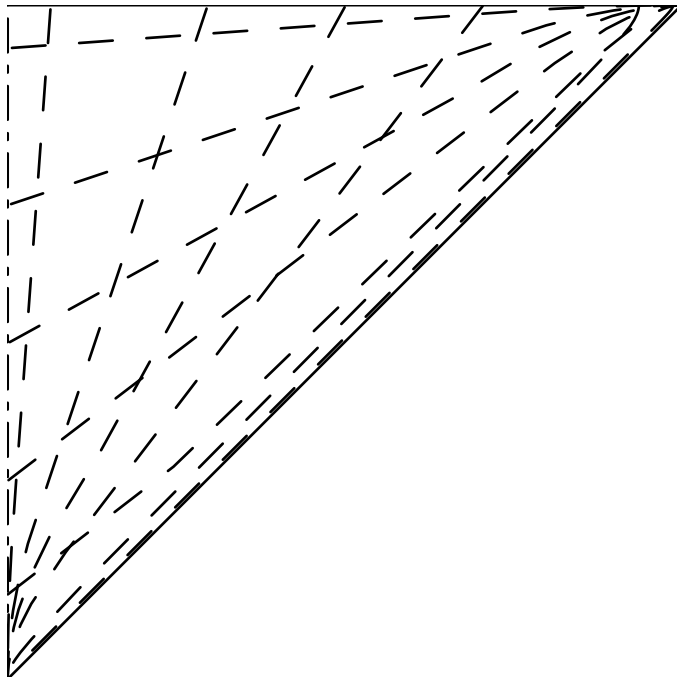


Figure 3—Flat Coordinates for de Sitter Space. The region covered by the flat coordinates is shown in a conformal diagram for all of maximally extended de Sitter space, identical to that in Fig. 2. Although the flat coordinates cover only half of maximally extended de Sitter space, the diagonal line, which is the boundary of the region covered by the flat coordinates, represents an initial value surface for all of de Sitter space.

To relate the flat and hyperbolic coordinates one can embed de Sitter space in (4+1)-dimensional Minkowski space as described in appendix A. Using $\sinh[t_h] = -1/\sinh[\eta]$,

$\cosh[t_h] = -\coth[\eta]$, and $\coth[t_h] = \cosh[\eta]$, one gets that the relation between the coordinate systems is

$$\begin{aligned} r_f &= \frac{\sinh[\xi]}{\cosh[\xi] + \cosh[\eta]}, \\ \eta_f &= \frac{\sinh[\eta]}{\cosh[\eta] + \cosh[\xi]}. \end{aligned} \tag{4.3}$$

The flat coordinates do not cover all of de Sitter space but only half of maximally extended de Sitter space, as indicated in the conformal diagram in Fig. 3. Nevertheless the flat coordinates cover enough of de Sitter space to contain an initial value surface for all of de Sitter space. The null surface indicated by the dashed diagonal line, the boundary of the region covered by the flat coordinates, is such a surface.[†]

To identify the hyperbolic modes of *positive* frequency with respect to the Bunch-Davies vacuum, it is convenient to use the null coordinates in the flat chart

$$\begin{aligned} u_f &= \eta_f + r_f, \\ v_f &= \eta_f - r_f. \end{aligned} \tag{4.4}$$

One has $v_f < 0$ and $|u_f| < -v_f$. We also define the region I hyperbolic null coordinates

$$\begin{aligned} U &= \eta + \xi, \\ V &= \eta - \xi \end{aligned} \tag{4.5}$$

where $V < 0$ and $|U| < -V$. Using the above relations between (η, ξ) and (η_f, r_f) one can see that two sets of null coordinates are related according to

$$U = \ln \left[\frac{1 + u_f}{1 - u_f} \right], \quad V = \ln \left[\frac{1 + v_f}{1 - v_f} \right]. \tag{4.6}$$

Conversely, $u_f = \tanh \frac{U}{2}$ and $v_f = \tanh \frac{V}{2}$. Thus we see that the region I hyperbolic coordinates only cover the region $-1 < v_f < 0$, $|u_f| < -v_f$ in terms of the flat coordinates.

[†] Technically, because this surface is null it is not a Cauchy surface, but initial data on this surface can be continued everywhere in de Sitter space.

The positive frequency modes with respect to open hyperbolic light cone coordinates in region I are

$$e^{-i\zeta U} = \left[\frac{1+u_f}{1-u_f} \right]^{-i\zeta}, \quad e^{-i\zeta V} = \left[\frac{1+v_f}{1-v_f} \right]^{-i\zeta}. \quad (4.7)$$

However, a full mode function for the Bunch-Davies vacuum must be specified in both regions I and V. A region I mode function must be continued into region V in order to calculate its inner product on the full space and the choice of analytic continuation distinguishes between positive and negative frequency Bunch-Davies modes. The identification of the positive frequency modes for the Bunch-Davies vacuum is determined by the analytic properties of the factors in $e^{-i\zeta U}$ and $e^{-i\zeta V}$ appearing in the hyperbolic mode functions above. The other factors in the hyperbolic mode functions contain only isolated singularities and no branch cuts, and thus will be seen to be irrelevant in making this identification. The bubble interior lies within the strip $-1 < u_f < +1$. Outside this strip one encounters a branch cut, taken here to lie near the real axis starting at $u_f = 1$, passing through $+\infty$, coming back from $-\infty$, and finally ending at $u_f = -1$, as indicated in Fig. 4. Thus $[(1+u_f)/(1-u_f)]^{i\zeta}$ has two possible continuations to the entire real line—one through the upper half-plane above the branch cut, and another through the lower half-plane below the branch cut.

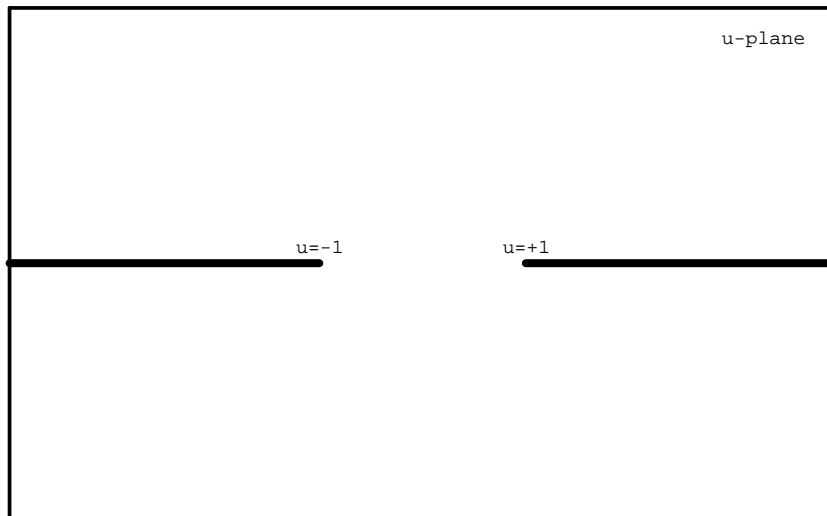


Figure 4—Analytic Continuation of the Mode Functions. The points $u_f = -1$ and $u_f = +1$ are branch points. To impose single-valuedness, we take a branch cut to start $u_f = +1$, extend to $u_f = +\infty$, come back from $u_f = +\infty$, and finally end at $u_f = -1$. The analytic continuation through the upper half-plane onto the remainder of the real line corresponds to the Bunch-Davies positive frequency modes. Similarly, the continuation through the lower half-plane corresponds to the Bunch-Davies negative frequency modes.

One can identify the positive frequency Bunch Davies modes by requiring they have vanishing overlap with the flat negative frequency modes $e^{i\omega u_f}$, ($\omega > 0$). Thus one requires

$$\int_{-\infty}^{+\infty} du_f e^{i\omega u_f} \left(\frac{1+u_f}{1-u_f} \right)^{i\zeta} = 0 \quad (4.8)$$

for all $\omega > 0$. This is satisfied by the analytic continuation through the upper half-plane above the branch cut, as deforming the contour toward $+i\infty$ makes this integral vanish. As a result, positive frequency Bunch Davies modes correspond to analytic continuation through the upper half plane into region V . This identification generalizes to gravitational wave hyperbolic modes and other more complicated mode functions of the form

$$R(u_f, v_f) \left(\frac{1+u_f}{1-u_f} \right)^{i\zeta} + S(u_f, v_f) \left(\frac{1+v_f}{1-v_f} \right)^{i\zeta} \quad (4.9)$$

where $R(u_f, v_f)$ and $S(u_f, v_f)$ are rational functions.

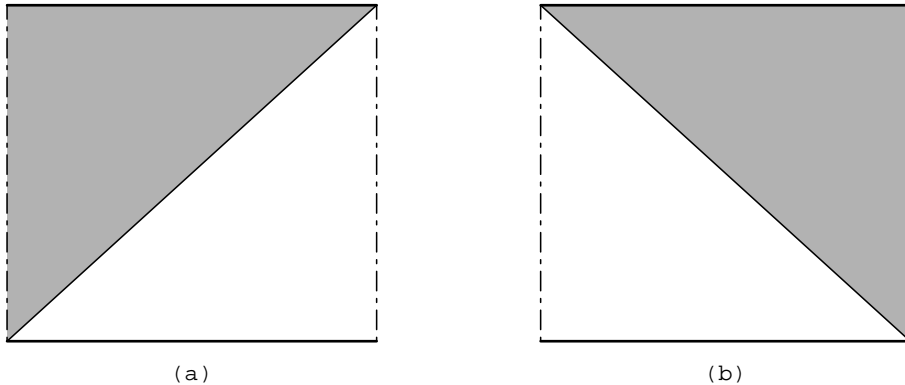


Figure 5—Dual Pair of Flat Coordinates. Both panels are conformal diagrams for maximally extended de Sitter space. The shaded triangle in Fig. 5(a) shows the region covered by the flat null coordinates (u_f, v_f) , while in Fig. 5(b) the region covered by null coordinates $(\tilde{u}_f, \tilde{v}_f)$, is shown.

We shall use two sets of flat coordinates (u_f, v_f) and $(\tilde{u}_f, \tilde{v}_f)$, as indicated in Fig. 5, related by a spatial reflection symmetry of de Sitter space that maps region I into region V. It may be shown that

$$\tilde{u}_f = \frac{-1}{v_f}, \quad \tilde{v}_f = \frac{-1}{u_f}, \quad (4.10)$$

either directly by using closed coordinates or by the analytic methods in appendix A.

This transformation relates the flat coordinates (u_f, v_f) covering the upper left triangular wedge of de Sitter space to the coordinates $(\tilde{u}_f, \tilde{v}_f)$ covering the upper right triangular wedge, as indicated in Fig. 5. As discussed earlier, for positive frequency mode functions the analytic continuation is with positive imaginary part, $(-1) = e^{i\pi}$, and so

$$\begin{aligned} \left(\frac{1+u_f}{1-u_f}\right)^{-i\zeta} &= \left((-1)^{-1} \frac{\tilde{1}+v_f}{1-\tilde{v}_f}\right)^{i\zeta} \equiv (-1)^{-i\zeta} e^{i\zeta\tilde{V}} \\ \left(\frac{1+v_f}{1-v_f}\right)^{-i\zeta} &= \left((-1)^{-1} \frac{\tilde{1}+u_f}{1-\tilde{u}_f}\right)^{i\zeta} \equiv (-1)^{-i\zeta} e^{i\zeta\tilde{U}}. \end{aligned} \quad (4.11)$$

As a result, positive hyperbolic frequency modes $e^{-i\zeta U}$, $e^{-i\zeta V}$ in region I become negative hyperbolic frequency modes in region V with an attenuation factor $e^{-\pi\zeta}$, and negative frequency region I hyperbolic modes become positive frequency hyperbolic modes in region V with an amplification factor $e^{\pi\zeta}$. The result of all this is that the positive frequency modes in region I are the modes proportional to $e^{iU\zeta}$, $e^{iV\zeta}$ for all values of ζ plus the continuation into region V using the upper half plane. The negative frequency modes are the same collection of modes with the opposite analytic continuation into region V.

We may normalize the modes by combining the fixed time surfaces of regions I and V. As shown in [14] for scalar subcurvature modes, and in the appendix for gravity waves, for the subcurvature modes under consideration here, the inner product is equivalent to that taken on a Cauchy surface for all of de Sitter space. Let $\mathcal{T}^{(I)}(\zeta, P, j, m)$ denote the modes with positive hyperbolic frequency in region I, as defined in eqn. (2.6), normalized using only the region I fixed time surface, and let $\mathcal{T}^{(V)}(\zeta, P, j, m)$ be the analogously defined modes in

region V. It follows that in region I one has the mode expansion,

$$\sum_{Pjm} \int_0^\infty \frac{d\zeta}{\sqrt{2\zeta(\zeta^2+1)}} \left\{ \left[\mathbf{T}^{Ejm}(\xi, \theta, \phi, \eta; \zeta) \right]_s^r \left[\frac{e^{+\pi\zeta/2}}{(e^{+\pi\zeta} - e^{-\pi\zeta})^{1/2}} T_h(\eta; \zeta) \hat{b}_I(\zeta, P, j, m) \right. \right. \\ \left. \left. + \frac{e^{-\pi\zeta/2}}{(e^{+\pi\zeta} - e^{-\pi\zeta})^{1/2}} T_h(\eta; -\zeta) \hat{b}_V(\zeta, P, j, m) \right] + h.c. \right\} \quad (4.12)$$

and similarly in region V

$$\sum_{jm} \int_0^\infty \frac{d\zeta}{\sqrt{2\zeta(\zeta^2+1)}} \left\{ \left[\mathbf{T}^{Ejm}(\xi, \theta, \phi, \eta; \zeta) \right]_s^r \left[\frac{e^{+\pi\zeta/2}}{(e^{+\pi\zeta} - e^{-\pi\zeta})^{1/2}} T_h(\eta; \zeta) \hat{b}_V(\zeta, P, j, m) \right. \right. \\ \left. \left. + \frac{e^{-\pi\zeta/2}}{(e^{+\pi\zeta} - e^{-\pi\zeta})^{1/2}} T_h(\eta; -\zeta) \hat{b}_I(\zeta, P, j, m) \right] + h.c. \right\} \quad (4.13)$$

where the annihilation operators $\hat{b}_I(\zeta, P, j, m)$ and $\hat{b}_V(\zeta, P, j, m)$ annihilate the Bunch-Davies vacuum for the graviton field and satisfy the usual commutation relations

$$\begin{aligned} [\hat{b}_A(\zeta, P, j, m), \hat{b}_B(\zeta', P', j', m')] &= 0, \\ [\hat{b}_A^\dagger(\zeta, P, j, m), \hat{b}_B^\dagger(\zeta', P', j', m')] &= 0, \\ [\hat{b}_A(\zeta, P, j, m), \hat{b}_B^\dagger(\zeta', P', j', m')] &= \delta_{AB} \delta(\zeta - \zeta') \delta_{PP'} \delta_{jj'} \delta_{mm'} \end{aligned} \quad (4.14)$$

where $(A, B = I, V)$. In the Bunch-Davies vacuum we observe a doubling in the number of modes. This reflects the existence of correlations between regions I and V—or, alternatively, between the inside and the outside of the bubble.

Another way of understanding this result for the vacuum is to note that the scalar mode functions and mixed tensor (with one raised and one lowered index, \mathcal{T}_B^A) mode functions considered here have the same time dependence. As the choice of vacuum depends only on the time dependence of the mode functions, the time dependence in the Bunch-Davies vacuum also has the same form for both cases.*

For the scalars there is a discrete vacuum mode [14] and here one also is normalizable, by the same arguments.

* J.D.C. thanks K. Schleich for discussions about this.

5. Gravity Waves and a Bubble with Finite Energy Difference

In this section we take into account the effects of the nonvanishing size of the critical bubble and of the nonvanishing difference in energy density across the bubble wall. In the presence of a bubble, one starts with a Bunch-Davies vacuum with $H = H_F$ as an initial condition outside the bubble and then continues these modes across the bubble wall into the open universe, where we idealize the expansion rate to be a constant with $H = H_T$. Of course, in realistic single-bubble inflationary models H inside the bubble is neither constant, nor does it correspond to the true vacuum as the subscript T suggests. However, in order to capture the qualitative consequences of changing H across the bubble wall without getting involved in the messy details of specific models, we consider the idealization of an infinitely thin wall, with constant $H = H_T$ inside, for calculating the gravitational waves. Whereas earlier in the paper we set H to unity, from here on factors of H will be displayed explicitly. Given that the gravity waves and the scalars have the same time dependence, and this is the only place the dependence on the wall appears, one can carry over the results for scalar fields. In the case at hand, we have a massless field before and after tunneling and a finite energy difference across the wall. The specific relevant results are from [18, 29, 21] and are briefly sketched below.

As will be shown below, any bubble with $H_F \neq H_T$ has a finite radius and extends outside the light cone (region I) covered by the $(\eta, \xi, \theta, \phi)$ coordinate system. By considering a curve of constant field value outside the light cone in Fig. 1a, one sees that the matching across the wall thus has to be done in region II and its Euclidean continuation. The continuation into region II from region I is $e^\eta \rightarrow -ie^{-u}$, $\xi \rightarrow \tau + i\pi/2$, and so the metric in region II becomes

$$ds^2 = a^2(u) \cdot \left[du^2 - d\tau^2 + \cosh^2 \tau d\Omega_{(2)}^2 \right]. \quad (5.1)$$

For an open universe $a(u) = 1/(H \cosh[u])$. The analytic continuation of the basis functions is given in somewhat more detail in appendix B and is straightforward. With the Euclidean continuation appropriate for tunneling, one also, before nucleation, rotates the space to Euclidean time $\tau \rightarrow i\tau_E$.

The wall has the same description in the Euclidean and Lorentzian regions in spacetime, since it only depends on u and not τ, τ_E . For a thin wall, the u dependent scale factor is [30]

$$a(u) = \begin{cases} \frac{1}{H_F \cosh[u]}, & \text{for } u < u_R, \\ \frac{1}{H_T \cosh[u+\delta]}, & \text{for } u > u_R, \end{cases} \quad (5.2)$$

where

$$\frac{1}{H_T \cosh[u+\delta]} = \frac{1}{H_F \left[\cosh[u - u_R] \cosh u_R + \sinh[u - u_R] \sqrt{\cosh^2[u_R] - (H_T/H_F)^2} \right]}. \quad (5.3)$$

The metrics are explicitly matched at the same value of $a(u)$, the bubble radius

$$R = \frac{1}{H_F \cosh[u_R]} = \frac{1}{H_T \cosh[u_R + \delta]}. \quad (5.4)$$

The mode functions in this background have only their u -dependence changing across the wall. Requiring continuity in the unchanged (τ, θ, ϕ) dependence forces the exterior mode functions to match onto interior modes with the same value of ζ^2 . To match the mode functions across this wall, we start with the initial u dependence corresponding to the analytic continuation of the time (η) dependence found in eqn. (2.11). As the exterior of the bubble has $H = H_F$, the false vacuum mode functions $e^{\pi\zeta/2} T_h(\eta \zeta)$, extend to region II as

$$A_\zeta(u) = H_F \cosh[u] e^{i\zeta u} \left(\tanh[u] - i\zeta \right) \quad (5.5)$$

up to a factor of i . These are matched across the wall onto modes of the *true* vacuum (as there is some slow roll after tunneling this is not exactly the true vacuum but is close enough for our purposes). The corresponding mode functions interior to the bubble, with $u > u_R$, $H = H_T$, are

$$B_\zeta(u + \delta) = H_T \cosh[u + \delta] e^{i\zeta(u+\delta)} \left(\tanh[u + \delta] - i\zeta \right). \quad (5.6)$$

Matching these and their first derivatives at the wall, at $a(u_R) = R$, gives

$$A_\zeta(u) = \alpha_\zeta B_\zeta(u + \delta) + \beta_\zeta B_{-\zeta}(u + \delta) \quad (5.7)$$

where

$$\begin{aligned}\alpha_\zeta &= \frac{2i\zeta - z}{2i\zeta} e^{-i\zeta\delta} \\ \beta_\zeta &= \frac{z}{2i\zeta} e^{i\zeta(2u_R + \delta)}\end{aligned}\tag{5.8}$$

and

$$z = \tanh[u_R] - \tanh[u_R + \delta] = \sqrt{1 - (H_F R)^2} - \sqrt{1 - (H_T R)^2}.\tag{5.9}$$

Note that these become trivial in the limit $\delta \rightarrow 0$, that is, when the energy difference $(H_F - H_T) \rightarrow 0$. From the definition of z , it appears possible that $z = 0$ is possible even if $H_F \neq H_T$, via taking $R = 0$. However, within the *new thin wall* approximation of [10], $R \propto \sqrt{H_F^2 - H_T^2}$ with a nonzero constant of proportionality, and in the usual thin wall approximation [31] one has that the radius obeys

$$R^2 = \frac{S_1^2}{c_0(H_F^2 - H_T^2) + c_1 S_1^2(H_F^2 + H_T^2) + c_2 S_1^4}\tag{5.10}$$

where S_1 is the surface tension (related to the integral of the change in the background field through the wall) and c_0, c_1, c_2 are positive constants. Since both H_F and H_T are finite and the surface tension does not vanish, R is finite.

One actually has to go to another coordinate system in order to show that there is a ‘time’ where there is only false vacuum and no bubble [30] for initial conditions. The consequence here is that the mode functions must be orthonormalized once they are continued across the bubble wall, as they do not correspond to a normalized initial mode functions in this other ‘time.’ Thus the mode functions given in eqn. (5.7) are not yet properly orthonormalized. At the nucleation time (conventionally taken as the $\tau = 0$ slice in region II), the whole system is rotated to Lorentzian signature. The mode functions can then be orthonormalized in region II, or since these are subcurvature modes, one can continue them to regions I and V and orthonormalize them there. The latter was done in detail in [18, 29] and the former was done in detail in [21]. Substituting the tensor rather than scalar spatial functions into these

results, in region II the wavefunction is, (again up to overall factors of i),

$$\begin{aligned}
h^r_s(\xi, \theta, \phi, \eta) &= \sum_{jm} \int_0^\infty \frac{d\zeta}{\sqrt{4\zeta(\zeta^2+1)} \sinh \pi\zeta} \left[\mathbf{T}^{Ejm}(\tau + i\pi/2, \theta, \phi, \eta; \zeta) \right]_s^r \\
&\times \left\{ \hat{b}_I(\zeta, E, j, m) \cdot \left[\left\{ C(+\zeta) \alpha_\zeta + S(+\zeta) \beta_{-\zeta} \right\} B_\zeta(u) \right. \right. \\
&\quad \left. \left. + \left\{ C(+\zeta) \beta_\zeta + S(+\zeta) \alpha_{-\zeta} \right\} B_{-\zeta}(u) \right] \right. \\
&\quad \left. + \hat{b}_V(\zeta, E, j, m) \cdot \left[\left\{ C(-\zeta) \alpha_{-\zeta} + S(-\zeta) \beta_\zeta \right\} B_{-\zeta}(u) \right. \right. \\
&\quad \left. \left. + \left\{ C(-\zeta) \beta_{-\zeta} + S(-\zeta) \alpha_\zeta \right\} B_\zeta(u) \right] \right\}. \tag{5.11}
\end{aligned}$$

As a result, the positive frequency part of the wavefunction inside region I for subcurvature modes is

$$\begin{aligned}
h^r_s(\xi, \theta, \phi, \eta) &= \sum_{jm} \int_0^\infty \frac{d\zeta}{\sqrt{2\zeta(\zeta^2+1)}} \left[\mathbf{T}^{Ejm}(\xi, \theta, \phi, \eta; \zeta) \right]_s^r \\
&\times \left\{ \hat{b}_I(\zeta, E, j, m) \cdot \left[\left\{ C(+\zeta) \alpha_\zeta + S(+\zeta) \beta_{-\zeta} \right\} \frac{e^{+\pi\zeta/2}}{(e^{+\pi\zeta} - e^{-\pi\zeta})^{1/2}} T_h(\eta; +\zeta) \right. \right. \\
&\quad \left. \left. + \left\{ C(+\zeta) \beta_\zeta + S(+\zeta) \alpha_{-\zeta} \right\} \frac{e^{-\pi\zeta/2}}{(e^{+\pi\zeta} - e^{-\pi\zeta})^{1/2}} T_h(\eta; -\zeta) \right] \right. \\
&\quad \left. + \hat{b}_V(\zeta, E, j, m) \cdot \left[\left\{ C(-\zeta) \alpha_{-\zeta} + S(-\zeta) \beta_\zeta \right\} \frac{e^{-\pi\zeta/2}}{(e^{+\pi\zeta} - e^{-\pi\zeta})^{1/2}} T_h(\eta; -\zeta) \right. \right. \\
&\quad \left. \left. + \left\{ C(-\zeta) \beta_{-\zeta} + S(-\zeta) \alpha_\zeta \right\} \frac{e^{+\pi\zeta/2}}{(e^{+\pi\zeta} - e^{-\pi\zeta})^{1/2}} T_h(\eta; +\zeta) \right] \right\} \tag{5.12}
\end{aligned}$$

where

$$\begin{aligned}
D_1(\zeta) &= \frac{1}{2} [|\alpha_\zeta|^2 + |\beta_\zeta|^2 + 1] = D_1(-\zeta) = 1 + \frac{z^2}{4\zeta^2}, \\
D_2(\zeta) &= \alpha_\zeta \beta_\zeta = \frac{-z}{4\zeta^2} (2i\zeta - z) e^{2i\zeta u_R}, \tag{5.13}
\end{aligned}$$

and

$$\begin{aligned}
C(\zeta) &= \sqrt{\frac{D_1}{D_1^2 - |D_2|^2}} \sqrt{\frac{1}{2} \left(1 + \sqrt{1 - \frac{|D_2|^2}{D_1^2}} \right)} = \sqrt{\frac{1}{2} \left(1 + \sqrt{\frac{4\zeta^2}{z^2 + 4\zeta^2}} \right)} \\
S(\zeta) &= \frac{-D_2}{|D_2|} \sqrt{\frac{D_1}{D_1^2 - |D_2|^2}} \sqrt{\frac{1}{2} \left(1 - \sqrt{1 - \frac{|D_2|^2}{D_1^2}} \right)} = \frac{-D_2}{|D_2|} \sqrt{\frac{1}{2} \left(1 - \sqrt{\frac{4\zeta^2}{z^2 + 4\zeta^2}} \right)}
\end{aligned}
\tag{5.14}$$

The identity $D_1^1 - |D_2|^2 = D_1$ was used in the above and can be checked by substituting into the definitions.

For scalars, an analogue of the vacuum supercurvature mode in the presence of a bubble, with $\zeta = -i$, remains normalizable when matched across the wall.^[29] This is true for the case here as well, but as this mode is η independent, it does not contribute to the CMB anisotropy below. Consequently we do not quote its value here.

6. Implications for the CMB Anisotropy

Gravitational waves provide a time dependent background for the photons in the CMB [32] (for a review see [33]). The contribution of gravitational waves to the CMB anisotropy is given by the integral in the Sachs–Wolfe formula [32]:

$$\begin{aligned}
\frac{\delta T_{gw}}{T(\Omega)} &= \frac{1}{2} \int_{\eta_e}^{\eta_0} d\eta \hat{r}^a \hat{r}^b \tilde{h}_{ab,\eta}(\xi = \eta_0 - \eta, \eta) \\
&= \frac{1}{2} \int_{\eta_e}^{\eta_0} d\eta \frac{\partial}{\partial \eta} \tilde{h}_{\xi\xi}(\xi = \eta_0 - \eta, \eta)
\end{aligned}
\tag{6.1}$$

The metric \tilde{h} is defined with the conformal factor scaled out, hence $\tilde{h}_{\mu\nu} = h_{\mu\nu}/a^2(\eta)$ in our notation. Here we have chosen the path to be parameterized by conformal time, where η_0 is the observing time and η_e is the last scattering time for the photon. The surface term vanishes for the tensor contribution and hence is omitted. The radial-radial component of the mode function has spatial dependence proportional to $F_j(\xi; \zeta)$, as seen in eqn. (3.4).

The Bunch-Davies positive frequency part of the temperature contrast operator is, using eqn. (5.12) from the last section,

$$\begin{aligned}
\frac{\delta T_{gw}^{(+)}(\Omega)}{T_{CMB}} &= \frac{1}{2} \sum_{jm} Y_{jm}(\Omega) \int_0^\infty d\zeta \frac{1}{\sqrt{2\zeta(\zeta^2+1)}} \int_{\eta_e}^{\eta_0} d\eta F_j(\xi = \eta_0 - \eta; \zeta) \\
&\times \left\{ \hat{b}_I(\zeta, E, j, m) \cdot \left[\left\{ C(+\zeta) \alpha_\zeta + S(+\zeta) \beta_{-\zeta} \right\} \frac{e^{+\pi\zeta/2}}{(e^{+\pi\zeta} - e^{-\pi\zeta})^{1/2}} \dot{T}_h(\eta; +\zeta) \right. \right. \\
&\quad \left. \left. + \left\{ C(+\zeta) \beta_\zeta + S(+\zeta) \alpha_{-\zeta} \right\} \frac{e^{-\pi\zeta/2}}{(e^{+\pi\zeta} - e^{-\pi\zeta})^{1/2}} \dot{T}_h(\eta; -\zeta) \right] \right. \\
&\quad \left. + \hat{b}_V(\zeta, E, j, m) \cdot \left[\left\{ C(-\zeta) \alpha_{-\zeta} + S(-\zeta) \beta_\zeta \right\} \frac{e^{-\pi\zeta/2}}{(e^{+\pi\zeta} - e^{-\pi\zeta})^{1/2}} \dot{T}_h(\eta; -\zeta) \right. \right. \\
&\quad \left. \left. + \left\{ C(-\zeta) \beta_{-\zeta} + S(-\zeta) \alpha_\zeta \right\} \frac{e^{+\pi\zeta/2}}{(e^{+\pi\zeta} - e^{-\pi\zeta})^{1/2}} \dot{T}_h(\eta; +\zeta) \right] \right\} \quad (6.2)
\end{aligned}$$

where the dots indicate derivative with respect to conformal time. The Bunch-Davies negative frequency component is

$$\frac{\delta T_{gw}^{(-)}(\Omega)}{T_{CMB}} = \left[\frac{\delta T_{gw}^{(+)}(\Omega)}{T_{CMB}} \right]^\dagger. \quad (6.3)$$

It is customary to expand the CMB anisotropy in terms of multipoles according to

$$\frac{\delta T_{gw}(\Omega)}{T_{CMB}} = \sum_{lm} a_{lm} Y_{lm}(\Omega). \quad (6.4)$$

The statistical average of the ensemble of classical gravity waves is found by taking the corresponding quantum average, so that the two-point correlation is

$$\begin{aligned}
c_l &= \langle |a_{lm}|^2 \rangle = \frac{1}{8} \int_0^\infty \frac{d\zeta}{\zeta(\zeta^2+1)} \int_{\eta_e}^{\eta_0} d\eta_1 \int_{\eta_e}^{\eta_0} d\eta_2 F_l(\xi = \eta_0 - \eta_1; \zeta) F_l(\xi = \eta_0 - \eta_2; \zeta) \\
&\times \left\{ \coth[\pi\zeta] \mathcal{R}e \left[\dot{T}_h(\eta_1; \zeta) \dot{T}_h(\eta_2; \zeta)^* \right] + \frac{1}{D_1 \sinh[\pi\zeta]} \mathcal{R}e \left[\alpha_\zeta \beta_{-\zeta} \dot{T}_h(\eta_1; \zeta) \dot{T}_h(\eta_2; \zeta) \right] \right\} \quad (6.5)
\end{aligned}$$

for all l . In showing this, it is useful to note that $|C(\zeta)|^2 + |S(\zeta)|^2 = 1$ and the definitions

in eqn. (5.13). Also since $D_1 = \frac{1}{2}[1 + |\alpha_\zeta|^2 + |\beta_\zeta|^2]$ and $|\alpha_\zeta|^2 - |\beta_\zeta|^2 = 1$,

$$\left| \frac{2\alpha_\zeta\beta_{-\zeta}}{1 + |\alpha_\zeta|^2 + |\beta_\zeta|^2} \right| \leq +1. \quad (6.6)$$

Consequently as one probes larger wavenumbers ζ (through larger- ℓ multipoles) the influence of the bubble dynamics quickly becomes negligible in a uniform manner. In other words, effects of the wall radius and finite energy difference rapidly disappear below the curvature scale, and thus are expected to be hidden in the cosmic variance, just as in the case for the scalar fluctuations.

The integrand in the eqn. (6.5) for the CMB multipole moments is well behaved for small ζ . This can be demonstrated with the explicit form of $F_2(\xi; \zeta)$ in eqn. (3.17). [Recall that for gravity waves the $\ell = 0, 1$ moments vanish because the graviton is a spin-two particle.] One then notes that F_j for higher j are obtained by taking derivatives, which will not alter the leading power of ζ (although the coefficients may change). As $\zeta \rightarrow 0$, the time dependence factor in the basis functions becomes

$$\partial_\eta T_h(\eta, \zeta) = \partial_\eta [(i\zeta \sinh[\eta] + \cosh[\eta])e^{-i\zeta\eta}] \rightarrow H_T \sinh[\eta] (1 - i\zeta\eta) + O(\zeta^2). \quad (6.7)$$

The first term in the curly brackets has the form

$$\begin{aligned} & \coth[\pi\zeta] \mathcal{R}e \left[\dot{T}_h(\eta_1; \zeta) \dot{T}_h(\eta_2; \zeta)^* \right] \\ &= \left(\frac{1}{\pi\zeta} \right) H_T^2 \sinh^2[\eta] (1 + O(\zeta^2)) \end{aligned} \quad (6.8)$$

since $\mathcal{R}e[1 - i\zeta(\eta_1 - \eta_2)] = 1$. For the second term in the curly brackets, for small ζ ,

$$\begin{aligned} & \frac{1}{D_1 \sinh[\pi\zeta]} \mathcal{R}e \left[\alpha_\zeta \beta_{-\zeta} \dot{T}_h(\eta_1; \zeta) \dot{T}_h(\eta_2; \zeta) \right] \\ &= \left[1 + \frac{z^2}{4\zeta^2} \right]^{-1} \frac{1 + O(\zeta^2)}{\pi\zeta} \mathcal{R}e \left[\alpha_\zeta \beta_{-\zeta} \dot{T}_h(\eta_1; \zeta) \dot{T}_h(\eta_2; \zeta) \right]. \end{aligned} \quad (6.9)$$

The argument in brackets on the right has the form

$$\begin{aligned} & \mathcal{R}e \left[\frac{2i\zeta - z}{2i\zeta} e^{-i\zeta(2\delta + 2u_r)} \frac{-z}{2i\zeta} [1 - i\zeta(\eta_1 + \eta_2) + O(\zeta^2)] \right] H_T^2 \sinh^2[\eta] \\ &= -\frac{z^2}{4\zeta^2} [1 + O(\zeta^2)] H_T^2 \sinh^2[\eta] \end{aligned} \quad (6.10)$$

including the small- ζ expansion of the exponentials. Thus, after factoring out the $H_T^2 \sinh^2[\eta]$ dependence, the term in curly brackets in eqn. (6.5) behaves as

$$\frac{1}{\pi\zeta} + \frac{\frac{-z^2}{4\zeta^2} + O(1)}{\pi\zeta(1 + \frac{z^2}{4\zeta^2})} \sim \zeta \quad (6.11)$$

for ζ small. In the Sachs-Wolfe integral above, we also have the factor of ζ^{-1} in the measure. Since $N_j \sim \zeta^{-2}$ one has (using eqn. (3.17) in conjunction with eqn. (3.27)) $F_j \sim \text{constant}$. This implies that the integrand approaches a constant as $\zeta \rightarrow 0$, rendering the integral infrared convergent.

As $(H_F - H_T)$ becomes small, both $\beta_{-\zeta}$ and z approach zero for fixed ζ , and the second term in curly brackets approaches zero. For vanishing z , as is found in the vacuum, eqn. (6.11) approaches $\coth[\pi\zeta]$, making the integrand appear to diverge as $\sim \zeta^{-2}$. We do not have an intuitive understanding of this limiting behavior. Vanishing z is never the case in the presence of the bubble since it implies exactly zero energy difference across the bubble wall.

In order to calculate the $a_{\ell m}$, one needs the time dependence of the wavefunctions from the inflationary period, through radiation domination and into the current phase of matter domination. Matching conditions have been found by [22] and are calculated analogously to the flat [1-7] and closed [34] universe cases. Time dependence has also been considered in [35] but seemingly for a different initial vacuum.

7. Discussion

We have determined the initial condition for the graviton field in an open universe originating from a bubble inflation model and calculated the contribution from gravitational waves to the CMB anisotropy. The total observed CMB anisotropy for a given multipole is obtained by combining in quadrature the gravity wave contribution calculated here with the scalar field contributions for the particular model. The effects of the bubble wall for the tensors, just as for the scalars, seems to be confined mostly to very large scales, corresponding to ζ small. It appears that the effects of curvature provide a much larger effect for the tensors than the effects of the wall.^[36]

Acknowledgements: We would like to thank R. Brandenberger, P. Ferreira, L. Ford, A. Guth, A. Liddle, A. Linde, B. Ratra, K. Schleich, N. Turok, and A. Vilenkin for useful discussions, and especially B. Allen and R. Caldwell for useful discussions and for sharing their prior unpublished manuscript^[22] with us. We thank R. Caldwell for comments on the draft. JDC is grateful in particular to M. White for numerous discussions and is supported by an ONR grant as a Mary Ingraham Bunting Institute Science Scholar. JDC also thanks the University of British Columbia, the Harvard-Smithsonian Center for Astrophysics, and the Center for Particle Astrophysics, the Physics Department, and LBNL at Berkeley for hospitality in the course of this work. MB was supported by the David and Lucille Packard Foundation and by National Science Foundation grant PHY 9309888.

Noted Added: After this work was completed we learned that Allen and Caldwell^[37] and Sasaki et al.^[38] have reached similar conclusions with respect to the influence of nonvanishing bubble size.

REFERENCES

1. L. Grishchuk, “The Amplification of Gravitational Waves and Creation of Gravitons in the Isotropic Universe,” *Lett. Nuovo Cimento* **12**, 60 (1975), Erratum: *Ibid.* **12**, 432 (1975); L. Grishchuk, “Amplification of Gravitational Waves in an Isotropic Universe,” *Zh. Eksp. Teor. Fiz.* **67**, 825 (1974). [Translation: *Sov. Phys. JETP* **40**, 409 (1975)].
2. A. Starobinsky, “A New Type of Isotropic Cosmological Models Without Singularity,” *Phys. Lett.* **B91**, 99 (1980); A. Starobinsky, “Relict Gravitation Radiation Spectrum and Initial State of the Universe,” *Pisma Zh. Eksp. Teor. Fiz.* **30**, 719 (1979) [Translation: *JETP Lett.* **30**, 682 (1979)].
3. L. Abbott and M. Wise, “Constraints on Generalized Inflationary Cosmologies,” *Nucl Phys.* **B244**, 541 (1984); L. Abbott and M. Wise, “Anisotropy of the Microwave Background in the Inflationary Cosmology,” *Phys. Lett.* **B135**, 279 (1984).
4. L. Abbott and R. Schaefer, “A General, Gauge-Invariant Analysis of the Cosmic Microwave Anisotropy,” *Ap. J.* **308**, 462 (1986).

5. L. Abbott and D. Harari, “Graviton Production in Inflationary Cosmology,” Nucl. Phys. **B264**, 487 (1986).
6. M. White, “Contribution of Long Wavelength Gravitational Waves to the Cosmic Microwave Background Anisotropy,” Phys. Rev. **D46**, 4198 (1992); B. Allen and S. Koranda, “CBR Anisotropy from Primordial Gravitational Waves in Inflationary Cosmologies,” Phys. Rev. **D50**, 3713 (1994).
7. L. Krauss and M. White, “Grand Unification, Gravitational Waves, and the Cosmic Microwave Background Anisotropy,” Phys. Rev. Lett. **69**, 869 (1992); R. Crittenden, J.R. Bond, R. Davis, G. Efstathiou, and P. Steinhardt, “The Imprint of Gravitational Waves on the Cosmic Microwave Background,” Phys. Rev. Lett. **71**, 324 (1993).
8. J.R. Gott, III, “Creation of Open Universes from de Sitter Space,” Nature **295**, 304 (1982); J.R. Gott and T. Statler, “Constraints on the Formation of Bubble Universes,” Phys. Lett. **136B**, 157 (1984); J.R. Gott, “Conditions for the Formation of Bubble Universes,” in E.W. Kolb et al., Eds., *Inner Space/Outer Space*, (Chicago: University of Chicago Press, 1986).
9. S. Coleman and F. de Luccia, “Gravitational Effects on and of Vacuum Decay,” Phys. Rev. **D21**, 3305 (1980).
10. M. Bucher, A.S. Goldhaber, and N. Turok, “An Open Universe From Inflation,” Phys. Rev. **D52**, 3314 (1995) (hep-ph 94-11206); M. Bucher and N. Turok, “Open Inflation with Arbitrary False Vacuum Mass,” Phys. Rev. **D52**, 3314 (1995) (hep-ph 95-03393).
11. M. Sasaki, T. Tanaka, K. Yamamoto, and J. Yokoyama, “Quantum State During and After Nucleation of an $O(4)$ Symmetric Bubble,” Prog. Theor. Phys. **90**, 1019 (1993); M. Sasaki, T. Tanaka, K. Yamamoto, and J. Yokoyama, “Quantum State Inside a Vacuum Bubble and Creation of an Open Universe,” Phys. Lett. **B317**, 510 (1993).
12. A. Linde, “Inflation with Variable Ω ,” Phys. Lett. **B351**, 99 (1995); A. Linde and A. Mezhlumian, “Inflation with $\Omega \neq 1$,” Phys. Rev. **D52**, 6789 (1995); L. Amendola, C. Baccigalupi, F. Occhionero, “Reconciling Inflation with Openness,” astro-ph/9504097 (1995); A. Green and A. Liddle, “Open Inflationary Universes in the Induced Gravity Theory,” astro-ph/9607166 (1996); J. Garcia-Bellido and A. Liddle, “Complete Power

- Spectrum for an Induced Gravity Open Inflation Model,” astro-ph/9610183 (1996).
13. B. Allen, “Vacuum States in de Sitter Space,” Phys. Rev. **D32**, 3136 (1985).
 14. M. Sasaki, T. Tanaka, and K. Yamamoto, “Euclidean Vacuum Mode Functions for a Scalar Field on Open de Sitter Space,” Phys. Rev. **D51**, 2979 (1995).
 15. D. Lyth and E. Stewart, “Inflationary Density Perturbations with $\Omega < 1$,” Phys. Lett. **B252**, 336 (1990).
 16. B. Ratra and P.J.E. Peebles, “Inflation in an Open Universe,” Phys. Rev. **D52**, 1837 (1995); B. Ratra and P.J.E. Peebles, “CDM Cosmogony in an Open Universe,” Ap. J. Lett. **432**, L5 (1994).
 17. K. Yamamoto, T. Tanaka, and M. Sasaki, “Particle Spectrum Created Through Bubble Nucleation and Quantum Field Theory in the Milne Universe,” Phys. Rev. **D51**, 2968 (1995).
 18. K. Yamamoto, T. Tanaka, and M. Sasaki, “Quantum Fluctuations and CMB Anisotropies in One-Bubble Open Inflation Models,” Phys. Rev. **D54**, 5031 (1996).
 19. T. Hamazaki, M. Sasaki, T. Tanaka, and K. Yamamoto, “Self Excitation of the Tunneling Scalar Field in False Vacuum Decay,” Phys. Rev. **D53**, 2045 (1996).
 20. J. Garriga and A. Vilenkin, “Perturbations on Domain Walls and Strings: A Covariant Theory,” Phys. Rev. **D44**, 1007 (1991); “Quantum Fluctuations on Domain Walls, Strings and Vacuum Bubbles,” Phys. Rev. **D45**, 3469 (1992); second reference of ref. 12 and ref. 19; J. Garriga, “Bubble fluctuations in $\Omega < 1$ inflation,” Phys. Rev. **D54**, 4764 (1996); J. Garcia-Bellido, “Density Perturbations from Quantum Tunneling in Open Inflation,” Phys. Rev. **D54**, 2473 (1996).
 21. J.D. Cohn, “Open Universes from Finite Radius Bubbles,” Phys. Rev. **D54**, 7215 (1996).
 22. B. Allen and R. Caldwell, “Cosmic Background Radiation Temperature Fluctuations in a Spatially Open Inflationary Universe,” (unpublished) (1994).
 23. R. Caldwell, private communication.

24. H. Kodama and M. Sasaki, “Cosmological Perturbation Theory,” *Prog. Theor. Phys. Suppl.* **78**, 1 (1984); V. Mukhanov, H. Feldman and R. Brandenberger, “Theory of Cosmological Perturbations,” *Phys. Rep.* **215**, 203 (1992).
25. T. Tanaka and M. Sasaki, “Quantized Gravitational Waves in the Milne Universe,” gr-qc/9610060 (1996), and also R. Caldwell, private communication.
26. K. Tomita, “Tensor Spherical and Psuedo-Spherical Harmonics in Four-Dimensional Spaces,” *Prog. Theor. Phys.* **68**, 310 (1982).
27. D. Lyth and A. Woszczyna, “Large Scale Perturbations in the Open Universe,” *Phys. Rev.* **D52**, 3338 (1995).
28. S.W. Hawking and G.F.R. Ellis, *The Large-Scale Structure of Space-Time*, (Cambridge: Cambridge University Press, 1973).
29. M. Sasaki and T. Tanaka, “Can the Simplest Two-Field Model of Open Inflation Survive”? astro-ph/9605104 (1996).
30. T. Tanaka and M. Sasaki, “Quantum State During and After O(4) Symmetric Bubble Nucleation with Gravitational Effects,” *Phys. Rev.* **D50**, 6444 (1994).
31. S. Parke, “Gravity and the Decay of the False Vacuum,” *Phys. Lett.* **121B**, 313 (1983).
32. R. Sachs and A. Wolfe, “Perturbations of a Cosmological Model and Angular Variation of the Microwave Background,” *Ap. J.* **147**, 73 (1967).
33. M. White, D. Scott, and J. Silk, “Anisotropies in the Cosmic Microwave Background,” *Ann. Rev. Astron. and Astrophys.* **32**, 319 (1994).
34. B. Allen, R. Caldwell, and S. Koranda, “CBR Temperature Fluctuations Induced by Gravitational Waves in a Spatially Closed Inflationary Universe,” *Phys. Rev.* **D51**, 1553 (1995).
35. M. R. de Garcia Maia and J.A.S. Lima, “Graviton Production in Elliptical and Hyperbolic Universes,” Brown-HET-1047, gr-qc/9606032 (1996).
36. W. Hu and M. White, to appear.
37. B. Allen and R. Caldwell, forthcoming paper.

38. M. Sasaki et al., astro-ph/9701053.
39. M. Bander and C. Itzykson, “Group Theory and the Hydrogen Atom (II),” *Rev. Mod. Phys.* **38**, 346 (1966).
40. N. Birrell and P. Davies, *Quantum Fields in Curved Space*, (Cambridge: Cambridge University Press, 1982), and references therein.
41. K. Thorne, “Multipole Expansions of Gravitational Radiation,” *Rev. Mod. Phys.* **52**, 299 (1980).
42. B. Allen, “Maximally Symmetric Spin Two Bitensors on S^3 and H^3 ,” *Phys. Rev.* **D51**, 5491 (1995).
43. U. H. Gerlach, “Thermal Ambience of Expanding Event Horizon in Minkowski Space-time,” *Phys. Rev.* **D28**, 761 (1983).
44. I. Redmount and S. Takagi, “Hyperspherical Rindler Space, Dimensional Reduction, and de Sitter Space Scalar Field Theory,” *Phys. Rev.* **D37**, 1443 (1988).

APPENDIX A—Relation Between Flat and Hyperbolic Coordinates

For the flat coordinates the line element is (setting $H = 1$)

$$ds^2 = -dt_f^2 + e^{2t_f} \cdot \left[dr_f^2 + r_f^2 d\Omega_{(2)}^2 \right] \quad (\text{A.1})$$

where $-\infty < t_f < +\infty$, or in terms of flat conformal time $\eta_f = -e^{-t_f}$

$$ds^2 = \frac{1}{\eta_f^2} \cdot \left[-d\eta_f^2 + d\eta_f^2 + r_f^2 d\Omega_{(2)}^2 \right]. \quad (\text{A.2})$$

To relate the flat and hyperbolic coordinates one can embed de Sitter space in (4+1)-dimensional Minkowski space (see ref. [10], section 5 or ref. [28]). The Minkowski coordinates

are $(\bar{w}, \bar{u}, \bar{x}, \bar{y}, \bar{z}) = (\bar{w}, \bar{u}, \bar{r})$ and de Sitter space is defined by

$$\bar{r}^2 + \bar{u}^2 - \bar{w}^2 = 1. \quad (\text{A.3})$$

The embedding of the open hyperbolic coordinates is

$$\begin{aligned} \bar{w} &= \sinh[t_h] \cosh[\xi], \\ \bar{u} &= \cosh[t_h], \\ \bar{r} &= \sinh[t_h] \sinh[\xi]. \end{aligned} \quad (\text{A.4})$$

Generally, $\bar{r} > 0$, and as $0 < t_h < \infty$ and $0 < \xi < \infty$, so that one sees that region I hyperbolic coordinates cover the range $0 \leq \bar{w} \leq \infty$, $1 \leq \bar{u}$. The flat coordinates are embedded in (4+1)-dimensional Minkowski space according to

$$t_f = \ln[\bar{w} + \bar{u}], \quad \eta_f = \frac{-1}{\bar{w} + \bar{u}}, \quad r_f = \frac{\bar{r}}{\bar{w} + \bar{u}}. \quad (\text{A.5})$$

These cover $\bar{w}, \bar{u} > 0$, a larger region than the hyperbolic open coordinates. As $\sinh[t_h] = -1/\sinh[\eta]$, $\cosh[t_h] = -\coth[\eta]$, and $\coth[t_h] = \cosh[\eta]$, the relation between the coordinate systems is

$$\begin{aligned} r_f &= \frac{\sinh[\xi]}{\cosh[\xi] + \cosh[\eta]}, \\ \eta_f &= \frac{\sinh[\eta]}{\cosh[\eta] + \cosh[\xi]}. \end{aligned} \quad (\text{A.6})$$

The flat coordinates do not cover all of de Sitter space but only half of maximally extended de Sitter space, as indicated in the conformal diagram in Fig. 3 in the text.

The null coordinates in the flat chart are

$$\begin{aligned} u_f &= \eta_f + r_f, \\ v_f &= \eta_f - r_f. \end{aligned} \quad (\text{A.7})$$

One has $v_f < 0$ and $|u_f| < |v_f|$. We also define the region I hyperbolic null coordinates

$$\begin{aligned} U &= \eta + \xi, \\ V &= \eta - \xi \end{aligned} \quad (\text{A.8})$$

where $V < 0$ and $|U| < |V|$. Using the above relations between (η, ξ) and (η_f, r_f) one can

show that the two sets of null coordinates are related according to

$$U = \ln \left[\frac{1 + u_f}{1 - u_f} \right], \quad V = \ln \left[\frac{1 + v_f}{1 - v_f} \right]. \quad (\text{A.9})$$

Conversely, $u_f = \tanh \frac{U}{2}$ and $v_f = \tanh \frac{V}{2}$. Thus we see that the hyperbolic coordinates cover only the region $|u_f|, |v_f| \leq 1$, $|u_f| \leq |v_f|$ in terms of the flat coordinates.

In order to see the continuation into region V, consider the transformation $u \rightarrow -u$ in the embedding Minkowski space. This can be accomplished by taking $t_h = -t_V - i\pi$. In terms of conformal time in region V, this is

$$\begin{aligned} \eta_V &= \ln \left[\tanh(-t_h/2 + i\pi/2) \right] = \ln(-1) + \ln \left[\tanh(t_h/2 - i\pi/2) \right] \\ &= \ln(-1) - \eta_h \end{aligned} \quad (\text{A.10})$$

Thus we have

$$\begin{aligned} \tilde{U} &= \eta_V + r_V = \ln(-1) - V \\ \tilde{V} &= \eta_V - r_V = \ln(-1) - U \end{aligned} \quad (\text{A.11})$$

where \tilde{U}, \tilde{V} are the hyperbolic open coordinates in region V. The definition of $\ln(-1)$ requires a choice of analytic continuation, which has been identified in terms of u_f, v_f , so converting to these coordinates, one has

$$\begin{aligned} u_f &= \tanh(U/2) = \tanh(-\tilde{V}/2 - \pm i\pi/2) = -\coth(\tilde{V}/2) = -\tilde{v}_f^{-1} \\ v_f &= \tanh(V/2) = \tanh(-\tilde{U}/2 - \pm i\pi/2) = -\coth(\tilde{U}/2) = -\tilde{u}_f^{-1} \end{aligned} \quad (\text{A.12})$$

as given in the text. This transformation relates the flat coordinates (u_f, v_f) covering the upper left triangular wedge of de Sitter space to the coordinates $(\tilde{u}_f, \tilde{v}_f)$ covering the upper right triangular wedge, as indicated in Fig. 5.

APPENDIX B—Inner Product in Region II

For this appendix, $H = 1$. To continue into region II, $e^\eta \rightarrow -ie^{-u}$, $\xi \rightarrow \tau + i\pi/2$, and the metric becomes

$$ds^2 = a^2(u) \left[du^2 - d\tau^2 + \cosh^2[\tau] d\Omega_{(2)}^2 \right] \quad (\text{B.1})$$

where $a(u) = 1/\cosh[u]$. The Wronskian, with respect to $-i\nabla_\tau$ on the symmetric perturbations of the metric, gives for an inner product

$$-\int_{\Sigma} \frac{du d\Omega \cosh^2[\tau]}{\cosh^2[u]} \mathcal{U}_A^B(\tau, \Sigma; \zeta, j, m) (i\overleftrightarrow{\partial}_\tau) \mathcal{U}_B^{A*}(\tau, \Sigma; \zeta', j', m') \quad (\text{B.2})$$

The Bunch-Davies vacuum mode expansion [see eqn. (4.12)] in region I

$$\begin{aligned} \sum_{Pjm} \int_0^\infty \frac{d\zeta}{\sqrt{2\zeta(\zeta^2+1)}} \left[\mathbf{T}^{Ejm}(\xi, \theta, \phi, \eta; \zeta) \right]_s^r & \left[\frac{e^{+\pi\zeta/2}}{(e^{+\pi\zeta} - e^{-\pi\zeta})^{1/2}} T_h(\eta; \zeta) \hat{b}_I(\zeta, P, j, m) \right. \\ & \left. + \frac{e^{-\pi\zeta/2}}{(e^{+\pi\zeta} - e^{-\pi\zeta})^{1/2}} T_h(\eta; -\zeta) \hat{b}_V(\zeta, P, j, m) \right] + h.c. \end{aligned} \quad (\text{B.3})$$

becomes in region II

$$\begin{aligned} \sum_{PJm} \int_0^\infty d\zeta & \left[\frac{e^{+\pi\zeta/2} n(\zeta)}{(e^{+\pi\zeta} - e^{-\pi\zeta})^{1/2}} T_h(\ln(-ie^{-u}); \zeta) T_A^B(\tau + i\frac{\pi}{2}, \theta, \phi; \zeta, j, m) \hat{b}_I(\zeta, P, J, m) \right. \\ & \left. + \frac{e^{-\pi\zeta/2} n(\zeta)}{(e^{+\pi\zeta} - e^{-\pi\zeta})^{1/2}} T_h(\ln(-ie^{-u}); -\zeta) [T_A^B(\tau + i\frac{\pi}{2}, \theta, \phi; \zeta, j, m)] \hat{b}_V(\zeta, P, J, m) \right] \\ & + h.c. \} \\ = \sum_{PJm} \int_0^\infty d\zeta & \{ \mathcal{U}_A^B(u, \tau, \theta, \phi; \zeta, j, m) \hat{b}_I(\zeta, P, J, m) + \mathcal{U}_A^B(u, \tau, \theta, \phi; -\zeta, j, m) \hat{b}_V(\zeta, P, J, m) \\ & + h.c. \} \end{aligned} \quad (\text{B.4})$$

Note that the complex conjugate is only taken in the u dependence in region II and both terms have the same τ dependence corresponding to positive frequency. The integral over

the surface Σ in region II is an integral over the analytic continuation of time u and over (θ, ϕ) . The analytic continuation of $T_h(\eta)$ multiplies the whole expression and is independent of τ . So for calculating the Wronskian, first consider only the τ dependence and the integral over θ, ϕ . The integral over u will be done subsequently. We have

$$\begin{aligned}
\tilde{\mathbf{T}}^{E,jm}(\tau, \theta, \varphi; \zeta) = & F_j(\tau + i\pi/2; \zeta) (\mathbf{e}^\tau \otimes \mathbf{e}^\tau) Y_{jm}(\theta, \varphi) \\
& + G_j(\tau + i\pi/2; \zeta) \delta_{\tilde{a}\tilde{b}} (\mathbf{e}^{\tilde{a}} \otimes \mathbf{e}^{\tilde{b}}) Y_{jm}(\theta, \varphi) \\
& + H_j(\tau + i\pi/2; \zeta) (\mathbf{e}^{\tilde{a}} \otimes \mathbf{e}^\tau + \mathbf{e}^\tau \otimes \mathbf{e}^{\tilde{a}}) \tilde{\nabla}_{\tilde{a}} Y_{jm}(\theta, \varphi) \\
& + I_j(\tau + i\pi/2; \zeta) (\mathbf{e}^{\tilde{a}} \otimes \mathbf{e}^{\tilde{b}}) \tilde{\nabla}_{\tilde{a}} \tilde{\nabla}_{\tilde{b}} Y_{jm}(\theta, \varphi)
\end{aligned} \tag{B.5}$$

Thus

$$\begin{aligned}
T_\tau^\tau &= -F_j(\tau + i\pi/2; \zeta) Y_{jm} \\
T_{\tilde{a}}^\tau &= -H_j(\tau + i\pi/2; \zeta) \tilde{\nabla}_{\tilde{a}} Y_{jm} \\
T_\tau^{\tilde{a}} &= \cosh^{-2}[\tau] H_j(\tau + i\pi/2; \zeta) \tilde{\nabla}^{\tilde{a}} Y_{jm} \\
T_{\tilde{b}}^{\tilde{a}} &= \cosh^{-2}[\tau] (I_j(\tau + i\pi/2; \zeta) \tilde{\nabla}^{\tilde{a}} \tilde{\nabla}_{\tilde{b}} Y_{jm} + \delta_{\tilde{b}}^{\tilde{a}} G_j(\tau + i\pi/2; \zeta) Y_{jm})
\end{aligned} \tag{B.6}$$

As we have $\nabla^2 Y_{jm} = -j(j+1)Y_{jm}$ and from earlier

$$\begin{aligned}
\int d\Omega (\nabla_{\tilde{a}} \nabla_{\tilde{b}} Y_{jm})^* \nabla^{\tilde{a}} \nabla^{\tilde{b}} Y_{j'm'} &= - \int d\Omega (\nabla^{\tilde{a}} \nabla_{\tilde{a}} \nabla_{\tilde{b}} Y_{jm})^* (\nabla^{\tilde{b}} Y_{j'm'}) \\
&= - \int d\Omega (\nabla_{\tilde{a}} \nabla_{\tilde{b}} \nabla^{\tilde{a}} Y_{jm})^* (\nabla^{\tilde{b}} Y_{j'm'}) \\
&= - \int d\Omega (\nabla_{\tilde{b}} \{ \nabla^2 + \frac{1}{2}R \} Y_{jm})^* (\nabla^{\tilde{b}} Y_{j'm'}) \\
&= [j(j+1)] \cdot [j(j+1) - 1] \delta_{jj'} \delta_{mm'} ,
\end{aligned} \tag{B.7}$$

we obtain immediately that

$$\begin{aligned}
\int d\Omega T_B^A \overleftrightarrow{\partial}_\tau T_A^{B*} &= \{ F_j \overleftrightarrow{\partial}_\tau F_j^* - 2j(j+1) \cosh^{-2}[\tau] H_j \overleftrightarrow{\partial}_\tau H_j^* \\
&\quad + \cosh^{-4}[\tau] (I_j \overleftrightarrow{\partial}_\tau I_j^* (j(j+1))(j(j+1) - 1) + 2G_j \overleftrightarrow{\partial}_\tau G_j^* \\
&\quad - j(j+1)(G_j \overleftrightarrow{\partial}_\tau I_j^* + I_j \overleftrightarrow{\partial}_\tau G_j^*)) \} \delta_{jj'} \delta_{mm'} \\
&= \{ \frac{3}{2} F_j \overleftrightarrow{\partial}_\tau F_j^* - 2j(j+1) \cosh^{-2}[\tau] H_j \overleftrightarrow{\partial}_\tau H_j^* \\
&\quad + \frac{1}{2} \cosh^{-4}[\tau] J^2 (J^2 - 2) I_j \overleftrightarrow{\partial}_\tau I_j^* \} \delta_{jj'} \delta_{mm'} .
\end{aligned} \tag{B.8}$$

The sign in front of H_j is due to the negative signature of τ . There is a factor of two in front

of both H_j and G_j . For H_j there is both a term T_{1a} as well as a term T_{a1} , and for G_j there is a contribution from both G_2 and G_3 . The minus sign in front of the last term is due to the negative sign relating ∇^2 and J^2 .

After some algebra, one finds that

$$\int d\Omega T_B^A \overleftrightarrow{\partial}_\tau T_A^{B*} = \frac{2\zeta^2(1+\zeta^2)\cosh^4[\tau]}{j(j+1)(j+2)(j-1)} F_j \overleftrightarrow{\partial}_\tau F_j^* \delta_{jj'} \delta_{mm'} \quad (\text{B.9})$$

After some work one can show that

$$F_j \overleftrightarrow{\partial}_\tau F_j^* = N_j(\zeta)^2 \frac{i \sinh[\pi\zeta]}{\cosh^6[\tau]} \zeta^3 (1+\zeta^2)(4+\zeta^2) \cdots (j^2+\zeta^2). \quad (\text{B.10})$$

Putting this all together and substituting for $N_j(\zeta)^2$, we get

$$\int d\Omega T_B^A \overleftrightarrow{\partial}_\tau T_A^{B*} = \frac{2i\zeta \sinh[\pi\zeta]}{\pi \cosh^2[\tau]} \delta_{jj'} \delta_{mm'} \quad (\text{B.11})$$

The integral over u remains, with mode functions

$$T_h(\ln(-ie^{-u}); \zeta) \frac{n(\zeta)e^{\frac{\pi\zeta}{2}}}{\sqrt{e^{+\pi\zeta} - e^{-\pi\zeta}}} = (i\zeta - \tanh[u]) e^{i\zeta u} \frac{\cosh[u] n(\zeta)}{\sqrt{(e^{\pi\zeta} - e^{-\pi\zeta})}}, \quad (\text{B.12})$$

so the last integral, including the rest of the measure, becomes

$$\begin{aligned} & \int du \frac{\cosh^2[\tau]}{\cosh^2[u]} \frac{\cosh[u](i\zeta - \tanh[u])n(\zeta)}{\sqrt{2 \sinh[\pi\zeta]}} \frac{\cosh[u](-i\zeta' - \tanh[u])n(\zeta')}{\sqrt{2 \sinh[\pi\zeta']}} e^{i(\zeta - \zeta')u} \\ &= \frac{2\pi \cosh^2[\tau]}{4\zeta \sinh[\pi\zeta]}. \end{aligned} \quad (\text{B.13})$$

As a result, we have

$$- \int_{\Sigma} du \cosh^{-2}[u] \cosh^2[\tau] \mathcal{U}_A^B(u, \Sigma; \zeta, j, m) (i \overleftrightarrow{\partial}_\tau) \mathcal{U}_B^{A*}(u, \Sigma; \zeta', j', m') = \delta(\zeta - \zeta') \delta_{jj'} \delta_{mm'} \quad (\text{B.14})$$

which agrees with eqn. (3.34).